viremia levels periodically in the same set of mice without sacrificing them, while most of the previously described SCID mouse models required mice to be sacrificed at each time point of testing (Mosier et al. 1993; Ruxrungtham et al. 1996; Strizki et al. 2001).

2.3 *Development of HSC-Engrafted Mouse for HIV-1 Infection*

Since human immune cells are not fully reconstituted in the chimeric mice transplanted with human PBMC, many researchers have been developing a improved immunodeficient mouse model engrafted with human HSC, which generates human T and B cells and also DC/macrophage myeloid cells for long periods of time and will be amenable to HIV-1 infection (Fig. 3). The HSC-engrafted mouse model allows mechanistic studies of HIV-1-induced disease progression, and possibly would allow analysis of immune responses derived from the human cells.

Using 8- to 10-week-old NOG mice engrafted with HSC or progenitor cells from cord blood, Nakahata and colleagues reported the significantly efficient reconstitution of human B cells as well as T cells in mice for more than 6 months (Hiramatsu et al. 2003). This successful engraftment (designated as the hNOG mouse) encouraged the subsequent HIV-1 infection experiment. We recently showed that in the hNOG mouse exhibiting long-lasting high levels of viremia and CD4 depletion in the peripheral blood were reproduced after both R5 and X4 HIV-1

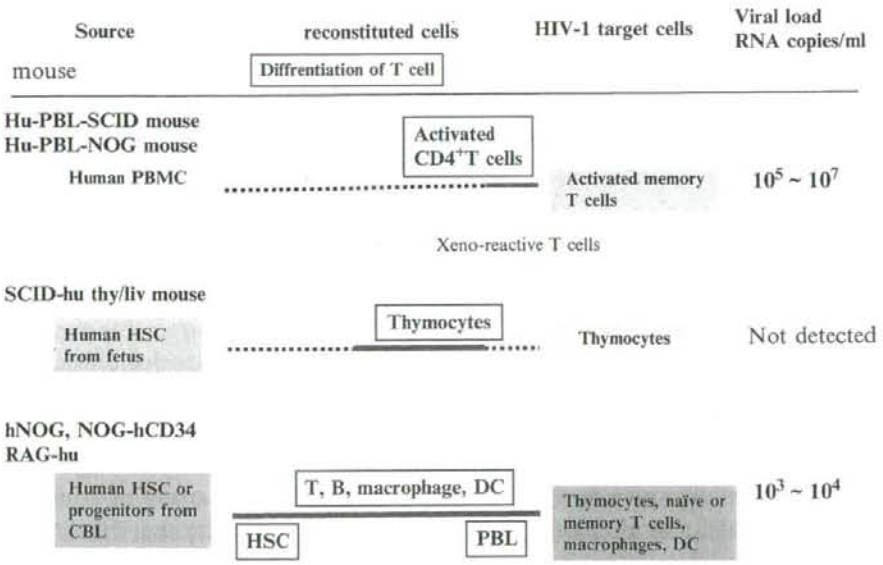

Fig. 3 Comparison of mouse/human chimeric models for HIV-1 infection. There have been three systems of humanized mouse models for HIV-1 infection

inoculation. Large amounts of HIV-1 DNA were detected in the spleen and bone marrow of R5 HIV-1-infected mice, and in the thymus and spleen of X4 virus-infected mice. Furthermore, anti-HIV p24 and gp120 antibodies were found in animals showing a high level of HIV-1 replication, indicating that HIV-1-specific immune response is induced in hNOG mice (Watanabe et al. 2007).

One modification of the CD34 engraftment into mice has been developed. Manz and colleagues reported that the newborn immunodeficient RAG-2/γ_c^{null} mouse strain is an adequate recipient for reconstitution of human immune cells including DC and that human adaptive immunity is clearly reconstituted in these mice (Traggiai et al. 2004). Another group also reported a significant improvement of human immune cell reconstitution with the newborn NOD/SCID/IL2 receptor γ chain^{null} mouse (Ishikawa et al. 2005). More recently, it was reported that efficient HIV-1 replication and CD4 depletion were shown in HSC-engrafted RAG-2/γ_c^{null} mice after HIV-1 inoculation (Baenziger et al. 2006; Berges et al. 2006; Zhang et al. 2007). We also confirmed that the engraftment procedure in newborn NOG mice with human CD34 created an HIV-1-susceptible mouse, and these mice (NOG-hCD34 mouse) after R5 or X4 HIV-1 inoculation possessed a level of viremia similar to that in HIV-1-infected patients. The NOG-hCD34 mice were also susceptible to infection with Epstein-Barr virus (EBV), which is known to be a human-specific γ herpes virus and to infect B cells. Several weeks after EBV inoculation, we could detect EBV DNA in the peripheral blood and spleen cells and could isolate EBV$^+$ lymphoblastoid cells from these mice (Koyanagi, unpublished observations).

3 Application of NOG Mice for HTLV Infection

3.1 HTLV

Human T-lymphotropic virus type I (HTLV-I) is another human retrovirus that causes adult T-cell leukemia (ATL)/ATL lymphoma and can also be involved in certain demyelinating diseases, tropical spastic paraparesis (TSP)/HTLV-I-associated myelopathy (HAM) (Hinuma et al. 1981; Osame et al. 1986). The malignant cells, mostly CD4$^+$ T cells, associated with all phases of ATL express very high levels of IL-2Rα (CD25) (Uchiyama et al. 1985). The median survival duration of all patients with aggressive ATL is about 13 months, and overall survival at 2 years is estimated to be about 30% (Taylor and Matsuoka 2005).

3.2 Model of HTLV-I-Induced Tumorigenicity

SCID mice have been utilized in a study on the pathomechanism and therapeutic strategy of ATL. Imada et al. examined the tumorigenicity of HTLV-I-infected cell

lines in an in vivo cell proliferation model using SCID mice. They found that 4 of 11 HTLV-I-infected cell lines were capable of proliferating in SCID mice after intraperitoneal inoculation. Interestingly, it was shown that some HTLV-I-infected and IL-2-dependent cell lines could be successfully engrafted in SCID mice (Imada et al. 1995). The expression of IL-2 mRNA was not detected in these cell lines growing either in vivo or in vitro. No HTLV-I viral structural proteins were detected in three of four transplantable cell lines proliferating in vivo. Peripheral blood T cells immortalized by introduction of *tax* gene of HTLV-I were found to have no tumorigenic potential in SCID mice. Although these systems were useful, two major drawbacks, namely, the long period of time required for tumor formation and the limitation of its use to certain cell lines, appear to hinder wider use of this animal model. These problems have now been overcome through development of the NOG mouse.

PBMC from patients with ATL were inoculated either intraperitoneally into the abdominal region or subcutaneously in the postauricular region of unconditional NOG mice. All mice developed clinical signs of near death, such as piloerection, weight loss, and cachexia, 6-8 weeks after inoculation of ATL cells in addition to enlargement of lymph nodes, spleen, lungs, and liver, whereas no tumors were found in the postauricular region or abdominal cavity where primary ATL cells were inoculated (Dewan et al. 2006). There was no difference in respect to the successful engraftment of ATL cells either intraperitoneally or subcutaneously inoculated into NOG mice. Histologic analysis of ATL-bearing mice showed massive infiltration of leukemic cells in various organs of NOG mice that were efficiently expressing human CD4 and CD25 molecules. A higher level of IL-2R (CD25) expression was observed on the surface of malignant cells associated with all stages of ATL as well as ATL cells infiltrated into various organs of patients. Thus, results from this model indicated successful engraftment and massive infiltration of primary ATL cells in various organs of NOG mice, like leukemia but without producing tumors at the sites of inoculation.

3.3 *Evaluation of Anti-*ATL *Compounds*

The various chemotherapies so far developed have not significantly increased the survival of patients with ATL (Taylor and Matsuoka 2005). Given the disappointing results using conventional chemotherapy, new approaches for the treatment of ATL are required. HTLV-I-infected cell lines derived from a leukemic cell clone and primary ATL cells failed to express significant amounts of Tax and other viral proteins, suggesting that the expression of viral proteins is not always necessary for leukemic proliferation at the late stage of the disease. However, HTLV-I-infected cell lines and leukemic cells from patients with ATL display constitutive NF-κB binding activity and increased degradation of a specific inhibitor, IκBα (Mori et al. 1999). NF-κB activation has been connected with multiple processes of oncogenesis, including control of apoptosis, cell cycle, differentiation, and cell migration; therefore, inhibition of NF-κB was suggested to be a useful strategy for cancer

therapy. Despite the diversity in clinical manifestations of ATL, strong and constitutive NF-κB activation was reported to be a unique and common characteristic of ATL cells (Mori et al. 1999). Thus, the indispensability of NF-κB for the maintenance of the malignant phenotype of HTLV-I provides a possible molecular target for ATL therapy. To study the effect of an NF-κB inhibitor, ritonavir, on ATL, we injected primary ATL cells from 10 patients subcutaneously into the postauricular region of NOG mice. Beginning 1 day after inoculation, mice were treated with either RPMI-1640 (as control) or ritonavir intraperitoneally daily for 30 days, followed by observation for another 30 days without any treatment. ATL cell inoculation promoted the development of piloerection, weight loss, and cachexia in addition to enlargement of lymph nodes, spleen, lungs, and liver in all control mice 2 months after inoculation. In contrast, ritonavir-treated mice were apparently healthy and had almost no enlargement of these organs. Clinical evaluation of organ invasion 2 months after injection of primary ATL cells showed that ritonavir treatment inhibited their infiltration into lymph nodes, spleen, lungs, and liver (Dewan et al. 2006). Seven of 10 patient samples injected in mice treated with ritonavir presented substantial inhibition of organ invasion, and 2 showed partial inhibition, whereas 1 sample failed to do so. In contrast, all control mice showed formation of new lymph nodes and infiltration with ATL cells into various organs. Organ infiltration of primary ATL cells was analyzed and evaluated by pathological staining and immunostaining of CD4 and CD25. We also performed similar experiments with HTLV-I-infected cell line cells [ED-40515(−), SLB-1, MT-1, TL-Oml, Hut-102, MT-2, and MT-4], using Bay 11-7082, which is another selective inhibitor of TNF-induced phosphorylation of IκBα without affecting the constitutive activation of IκBα phosphorylation, eventually resulting in decreased NF-κB and decreased expression of adhesion molecules (Dewan et al. 2003). Essentially, the same results were obtained in the studies using BAY11-7082 and the ED-40515(−) cell line. Together, these data indicate that NF-κB antagonists significantly inhibit ATL cell growth and infiltration in various organs of NOG mice.

Our NOG ATL model presents many features 6-8 weeks after inoculation of ATL cells such as the clinical signs observed in patients with ATL. Two clinical types, acute and chronic, carry very different prognoses. However, no difference in cell growth, surface phenotype, and NF-κB activity is observed in primary leukemic cells from patients with acute- and chronic-type ATL. Therefore, the same characteristics of freshly isolated ATL cells with acute- and chronic-type were observed in the NOG mouse. Thus, it represents a novel model to evaluate tissue toxicity and the efficacy of therapeutic agents directed toward the treatment of ATL (Fig. 4).

4 Concluding Remarks on Human Retrovirus Infection Model

The humanized mouse model should provide a midway position between the laboratory and clinical studies. From a relevant animal model for HIV and HTLV infections, immunological as well as virological aspects of the disease could be

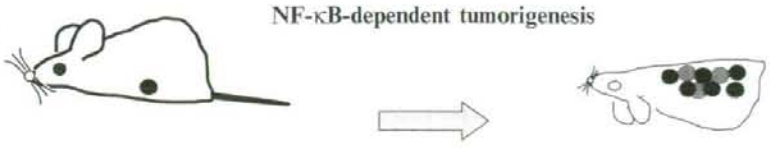

Clinical signs in NOG ATL model
Development to $CD4^+CD25^+$ lymphoma
Invasion of leukemic cells to multiple organs
Cachexia
No expression of HTLV-I proteins

Fig. 4 NOG ATL model. Model of HTLV-I-induced tumorigenicity is created with NOG mice. $HTLV^+$ T cells as well as primary ATL leukemic cells induce the identical clinical signs observed in patients with ATL

investigated, and such an animal model could be used to examine the disease process and efficacy of antiviral compounds or vaccines. Significant progress in creating refined mouse strains has been achieved. We have now humanized mice, animals that circulate human blood. However, a mouse is not human. Therefore, there are still many limitations for examination of the human defense system. It is expected that the developments of technology in experimental animals and embryology, including methods using human ES or some other progenitor cells, will open the new evolution of humanized animals.

Acknowledgements This work was supported by grants from the Ministry of Health, Labor and Welfare, and the Ministry of Education, Culture, Sports, Science and Technology of Japan.

References

Aldrovandi GM, Feuer G, Gao L, Jamieson B, Kristeva M, Chen IS, Zack JA (1993) The SCID-hu mouse as a model for HIV-1 infection. Nature 363:732-736

Baenziger S, Tussiwand R, Schlaepfer E, Mazzucchelli L, Heikenwalder M, Kurrer MO, Behnke S, Frey J, Oxenius A, Joller H, Aguzzi A, Manz MG, Speck RF (2006) Disseminated and sustained HIV infection in CD34+ cord blood cell-transplanted Rag2–/–gamma c–/– mice. Proc Natl Acad Sci USA 103:15951-15956

Berges BK, Wheat WH, Palmer BE, Connick E, Akkina R (2006) HIV-1 infection and CD4 T cell depletion in the humanized Rag2–/–gamma c–/– (RAG-hu) mouse model. Retrovirology 3:76

Blunt T, Finnie NJ, Taccioli GE, Smith GC, Demengeot J, Gottlieb TM, Mizuta R, Varghese AJ, Alt FW, Jeggo PA et al. (1995) Defective DNA-dependent protein kinase activity is linked to VDJ recombination and DNA repair defects associated with the murine scid mutation. Cell 80:813-823

Bonyhadi ML, Rabin L, Salimi S, Brown DA, Kosek J, McCune JM, Kaneshima (1993) HIV induces thymus depletion in vivo. Nature 363:728-732

Bosma GC, Custer RP, Bosma MJ (1983) A severe combined immunodeficiency mutation in the mouse. Nature 301:527-530

Boubnov NV, Weaver DT (1995) scid cells are deficient in Ku and replication protein A phosphorylation by the DNA-dependent protein kinase. Mol Cell Biol 15:5700-5706

Delhem N, F Hadida, G Gorochov, F Carpentier, JP de Cavel, JF Andreani, B Autran, JY Cesbron (1998) Primary Th1 cell immunization against HIVgp160 in SCID-hu mice coengrafted with peripheral blood lymphocytes and skin. J Immunol 161:2060-2069

Dewan MZ, Terashima K, Taruishi M, Hasegawa H, Ito M, Tanaka Y, Mori N, Sata T, Koyanagi Y, Maeda M, Kubuki Y, Okayama A, Fujii M, Yamamoto N (2003) Rapid tumor formation of human T-cell leukemia virus type 1-infected cell lines in novel NOD-SCID/γc^{null} mice: suppression by an inhibitor against NF-kappaB. J Virol 77:5286-5294

Dewan MZ, Uchihara JN, Terashima K, Honda M, Sata T, Ito M, Fujii N, Uozumi K, Tsukasaki K, Tomonaga M, Kubuki Y, Okayama A, Toi M, Mori N, Yamamoto N (2006) Efficient intervention of growth and infiltration of primary adult T-cell leukemia cells by an HIV protease inhibitor, ritonavir. Blood 107:716-724

Gorantla S, Santos K, Meyer V, Dewhurst S, Bowers WJ, Federoff HJ, Gendelman HE, Poluektova L (2005) Human dendritic cells transduced with herpes simplex virus amplicons encoding human immunodeficiency virus type 1 (HIV-1) gp120 elicit adaptive immune responses from human cells engrafted into NOD/SCID mice and confer partial protection against HIV-1 challenge. J Virol 79:2124-2132

Hartley O, Gaertner H, Wilken J, Thompson D, Fish R, Ramos A, Pastore C, Dufour B, Cerini F, Melotti A, Heveker N, Picard L, Alizon M, Mosier D, Kent S, Offord R (2004) Medicinal chemistry applied to a synthetic protein: development of highly potent HIV entry inhibitors. Proc Natl Acad Sci USA 101:16460-16465

Hinuma Y, Nagata K, Hanaoka M, Nakai M, Matsumoto T, Kinoshita KI, Shirakawa S, Miyoshi I (1981) Adult T-cell leukemia: antigen in an ATL cell line and detection of antibodies to the antigen in human sera. Proc Natl Acad Sci USA 78:6476-6480

Hiramatsu H, Nishikomori R, Heike T, Ito M, Kobayashi K, Katamura K, Nakahata T (2003) Complete reconstitution of human lymphocytes from cord blood CD34+ cells using the NOD/SCID/γ_c^{null} mice model. Blood 102:873-880

Ifversen P, Borrebaeck CA (1996) SCID-hu-PBL: a model for making human antibodies? Semin Immunol 8:243-248

Imada K, Takaori-Kondo A, Akagi T, Shimotohno K, Sugamura K, Hattori T, Yamabe H, Okuma M, Uchiyama T (1995) Tumorigenicity of human T-cell leukemia virus type I-infected cell lines in severe combined immunodeficient mice and characterization of the cells proliferating in vivo. Blood 86:2350-2357

Ishikawa F, Yasukawa M, Lyons B, Yoshida S, Miyamoto T, Yoshimoto G, Watanabe T, Akashi K, Shultz LD, Harada M (2005) Development of functional human blood and immune systems in γ chain^{null} mice. Blood 106:1565-1573

Ito M, Hiramatsu H, Kobayashi K, Suzue K, Kawahata M, Hioki K, Ueyama Y, Koyanagi Y, Sugamura K, Tsuji K, Heike T, Nakahata T (2002) NOD/SCID/γ_c^{null} mouse: an excellent recipient mouse model for engraftment of human cells. Blood 100:3175-3182

Jamieson BD, Zack JA (1999) Murine models for HIV disease. AIDS 13 Suppl A:S5-11

Kaneshima H, Shih CC, Namikawa R, Rabin L, Outzen H, Machado SG, McCune JM (1991) Human immunodeficiency virus infection of human lymph nodes in the SCID/hu mouse. Proc Natl Acad Sci USA 88:4523-4527

Kaneshima H, Su L, Bonyhadi ML, Connor RI, Ho DD, McCune JM (1994) Rapid-high, syncytium-inducing isolates of human immunodeficiency virus type 1 induce cytopathicity in the human thymus of the SCID-hu mouse. J Virol 68:8188-8192

Kawano Y, Tanaka Y, Misawa N, Tanaka R, Kira JI, Kimura T, Fukushi M, Sano K, Goto T, Nakai M, Kobayashi T, Yamamoto N, Koyanagi Y (1997) Mutational analysis of human immunodeficiency virus type 1 (HIV-1) accessory genes: requirement of a site in the nef gene for HIV-1 replication in activated CD4+ T cells in vitro and in vivo. J Virol 1:8456-8466

Kirchgessner CU, Patil CK, Evans JW, Cuomo CA, Fried LM, Carter T, Oettinger MA, Brown JM (1995) DNA-dependent kinase (p350) as a candidate gene for the murine SCID defect. Science 267:1178-1183

Koyanagi Y, Tanaka Y, Kira J, Ito M, Hioki K, Misawa N, Kawano Y, Yamasaki K, Tanaka R, Suzuki Y, Ueyama Y, Terada E, Tanaka T, Miyasaka M, Kobayashi T, Kumazawa Y, Yamamoto N (1997a) Primary human immunodeficiency virus type 1 viremia and central nervous system invasion in a novel hu-PBL-immunodeficient mouse strain. J Virol 71:2417-2424

Koyanagi Y, Tanaka Y, Tanaka R, Misawa N, Kawano Y, Tanaka T, Miyasaka M, Ito M, Ueyama Y, Yamamoto N (1997b) High levels of viremia in hu-PBL-NOD-scid with HIV-1 infection. Leukemia 11 Suppl 3:109-112

Lu W, LC Arraes, WT Ferreira, J-M Andrieu (2004) Therapeutic dendritic-cell vaccine for chronic HIV-1 infection. Nat Med 10:1359-1365

Lu W, X Wu, Y Lu, W Guo, JM Andrieu (2003) Therapeutic dendritic-cell vaccine for simian AIDS. Nat Med 9:27-32

McCune JM, Kaneshima H, Krowka J, Namikawa R, Outzen H, Peault B, Rabin L, Shih CC, Yee E, Lieberman M et al. (1988) The SCID-hu mouse: murine model for the analysis of human hematolymphoid differentiation and function. Science 241:1632-1639

McCune JM, Kaneshima H, Krowka J, Namikawa R, Outzen H, Peault B, Rabin L, Shih CC, Yee E, Lieberman M et al. (1991) The SCID-hu mouse: a small animal model for HIV infection and pathogenesis. Annu Rev Immunol 9:399-429

McCune JM, Namikawa R, Shih CC, Rabin L, Kaneshima H (1990) Suppression of HIV infection in AZT-treated SCID/hu mice. Science 247:564-566

Miller RD, Hogg J, Ozaki JH, Gell D, Jackson SP, Riblet R (1995) Gene for the catalytic subunit of mouse DNA-dependent protein kinase maps to the scid locus. Proc Natl Acad Sci USA 92:10792-10795

Miura Y, Misawa N, Kawano Y, Okada H, Inagaki Y, Yamamoto N, Ito M, Yagita H, Okumura K, Mizusawa H, Koyanagi Y (2003) Tumor necrosis factor-related apoptosis-inducing ligand induces neuronal death in a murine model of HIV central nervous system infection. Proc Natl Acad Sci USA 100:2777-2782

Miura Y, Misawa N, Maeda N, Inagaki Y, Tanaka Y, Ito M, Kayagaki N, Yamamoto N, Yagita H, Mizusawa H, Koyanagi Y (2001) Critical contribution of TNF-related apoptosis-inducing ligand (TRAIL) to apoptosis of human $CD4^+$ T cells in HIV-1-infected hu-PBL-NOD-SCID mice. J Exp Med 193:651-659

Mori N, Fujii M, Ikeda S, Yamada Y, Tomonaga M, Ballard DW, Yamamoto N (1999) Constitutive activation of NF-kappaB in primary adult T-cell leukemia cells. Blood 93:2360-2368

Mosier DE, Gulizia RJ, Baird SM, Wilson DB (1988) Transfer of a functional human immune system to mice with severe combined immunodeficiency. Nature 335:256-259

Mosier DE, Gulizia RJ, Baird SM, Wilson DB, Spector DH, Spector SA (1991) Human immunodeficiency virus infection of human-PBL-SCID mice. Science 251:791-794

Mosier DE, Gulizia RJ, MacIsaac PD, Torbett BE, Levy JA (1993) Rapid loss of CD4+ T cells in human-PBL-SCID mice by noncytopathic HIV isolates. Science 260:689-692

Nakata H, Maeda K, Miyakawa T, Shibayama S, Matsuo M, Takaoka Y, Ito M, Koyanagi Y, Mitsuya H (2005) Potent Anti-R5-human immunodeficiency virus type 1 effects of a CCR5 antagonist, AK602/ONO4128/GW873140, in a novel human peripheral blood mononuclear cell nonobese diabetic-SCID, interleukin 2 receptor γ-chain-knocked-out AIDS mouse model. J Virol 79: 2087-2096

Namikawa R, Kaneshima H, Lieberman M, Weissman IL, McCune JM (1988) Infection of the SCID-hu mouse by HIV-1. Science 242:1684-1686

Nimura F, Zhang LF, Okuma K, Tanaka R, Sunakawa H, Yamamoto N, Tanaka Y. (2006) Cross-linking cell surface chemokine receptors leads to isolation, activation, and differentiation of monocytes into potent dendritic cells. Exp Biol Med 231:431-443

Nonoyama S, Smith FO, Ochs HD (1993) Specific antibody production to a recall or a neoantigen by SCID mice reconstituted with human peripheral blood lymphocytes. J Immunol. 151:3894-3901

Osame M, Usuku K, Izumo S, Ijichi N, Amitani H, Igata A, Matsumoto M, Tara M (1986) HTLV-I associated myelopathy, a new clinical entity. Lancet 1:1031-1032

Pastore C, Picchio GR, Galimi F, Fish R, Hartley O, Offord RE, Mosier DE (2003) Two mechanisms for human immunodeficiency virus type 1 inhibition by N-terminal modifications of RANTES. Antimicrob Agents Chemother 47:509-517

Peterson SR, Kurimasa A, Oshimura M, Dynan WS, Bradbury EM, Chen DJ (1995) Loss of the catalytic subunit of the DNA-dependent protein kinase in DNA double-strand-break-repair mutant mammalian cells. Proc Natl Acad Sci USA 92:3171-3174

Rabin L, Hincenbergs M, Moreno MB, Warren S, Linquist V, Datema R, Charpiot B, Seifert J, Kaneshima H, McCune J (1996) Use of standardized SCID/hu Thy/Liv mouse model for preclinical efficacy testing of anti-human immunodeficiency virus type 1 compounds. Antimicrob Agents Chemother 40:755-762

Ruxrungtham K, Boone E, Ford H Jr, Driscoll JS, Davey RT Jr, Lane HC (1996) Potent activity of 2'-beta-fluoro-2',3'-dideoxyadenosine against human immunodeficiency virus type 1 infection in hu-PBL-SCID mice. Antimicrob Agents Chemother 40:2369-2374

Sandhu JS, Gorczynski R, Shpitz B, Gallinger S, Nguyen HP, Hozumi N (1995) A human model of xenogeneic graft-versus-host disease in SCID mice engrafted with human peripheral blood lymphocytes. Transplantation 60:179-184

Sandhu JS, Shpitz B, Gallinger S, Hozumi N (1994) Human primary immune response in SCID mice engrafted with human peripheral blood lymphocytes. J Immunol 152:3806-3813

Santini S M, C Lapenta, M Logozzi, S Parlato, M Spada, T Di Pucchio, F Belardelli (2000) Type I interferon as a powerful adjuvant for monocyte-derived dendritic cell development and activity in vitro and in Hu-PBL-SCID mice. J Exp Med 191:1777-1788

Stanley SK, McCune JM, Kaneshima H, Justement JS, Sullivan M, Boone E, Baseler M, Adelsberger J, Bonyhadi M, Orenstein J et al. (1993) Human immunodeficiency virus infection of the human thymus and disruption of the thymic microenvironment in the SCID-hu mouse. J Exp Med 178:1151-1163

Strizki JM, Xu S, Wagner NE, Wojcik L, Liu J, Hou Y, Endres M, Palani A, Shapiro S, Clader JW, Greenlee WJ, Tagat JR, McCombie S, Cox K, Fawzi AB, Chou CC, Pugliese-Sivo C, Davies L, Moreno ME, Ho DD, Trkola A, Stoddart CA, Moore JP, Reyes GR, Baroudy BM (2001) SCH-C (SCH 351125), an orally bioavailable, small molecule antagonist of the chemokine receptor CCR5, is a potent inhibitor of HIV-1 infection in vitro and in vivo. Proc Natl Acad Sci USA 98:12718-12723

Tary-Lehmann M and Saxon A (1992) Human mature T cells that are anergic in vivo prevail in SCID mice reconstituted with human peripheral blood. J Exp Med 175:503-516

Tary-Lehmann M, Saxon A, Lehmann PV (1995) The human immune system in hu-PBL-SCID mice. Immunol Today 16:529-533

Taylor GP, Matsuoka M (2005) Natural history of adult T-cell leukemia/lymphoma and approaches to therapy. Oncogene 24:6047-6057

Traggiai E, Chicha L, Mazzucchelli L, Bronz L, Piffaretti JC, Lanzavecchia A, Manz MG (2004) Development of a human adaptive immune system in cord blood cell-transplanted mice. Science 304:104-107

Uchiyama T, Hori T, Tsudo M, Wano Y, Umadome H, Tamori S, Yodoi J, Maeda M, Sawami H, Uchino H (1985) Interleukin-2 receptor (Tac antigen) expressed on adult T cell leukemia cells. J Clin Invest 76:446-453

Vandekerckhove BA, Namikawa R, Bacchetta R, Roncarolo MG (1992) Human hematopoietic cells and thymic epithelial cells induce tolerance via different mechanisms in the SCID-hu mouse thymus. J Exp Med 175:1033-1043

Watanabe S, Terashima K, Ohta S, Horibata S, Yajima M, Shiozawa Y, Dewan MZ, Yu Z, Ito M, Morio T, Shimizu N, Honda M, Yamamoto N (2007) Hematopoietic stem cell-engrafted NOD/SCID/IL2Rgamma null mice develop human lymphoid systems and induce long-lasting HIV-1 infection with specific humoral immune responses. Blood 109:212-218

Yoshida A, Tanaka R, Kodama A, Yamamoto N, Ansari AA, Tanaka Y (2005) Identification of HIV-1 epitopes that induce the synthesis of a R5 HIV-1 suppression factor by human CD4+ T cells isolated from HIV-1 immunized hu-PBL SCID mice. Clin Dev Immunol 12:235-242

Yoshida A, Tanaka R, Murakam M, Takahashi T, Koyanagi Y, Nakamura M, Ito M, Yamamoto N, Tanaka Y (2003) Induction of protective immune responses against R5 HIV-1 infection in the hu-PBL-SCID mice by intra-splenic immunization with HIV-1-pulsed dendritic cells: possible involvement of a novel factor of human CD4+ T cell origin. J Virol 77:8719-8728

Zhang L, Kovalev GI, Su L (2007) HIV-1 infection and pathogenesis in a novel humanized mouse model. Blood 109:2978-2981

JOURNAL OF VIROLOGY, Jan. 2008, p. 1021–1033 Vol. 82, No. 2
0022-538X/08/$08.00+0 doi:10.1128/JVI.01044-07

Modulation of Human Immunodeficiency Virus Type 1 Infectivity through Incorporation of Tetraspanin Proteins▽

Kei Sato,[1] Jun Aoki,[1,2] Naoko Misawa,[1] Eriko Daikoku,[3] Kouichi Sano,[3] Yuetsu Tanaka,[4] and Yoshio Koyanagi[1]*

Laboratory of Viral Pathogenesis, Institute for Virus Research, Kyoto University, Sakyo-ku, Kyoto, Kyoto 606-8507, Japan[1]; Department of Immunology, Tohoku University Graduate School of Medicine, Aoba-ku, Sendai, Miyagi 980-8575, Japan[2]; Department of Preventive and Social Medicine, Osaka Medical College, Takatsuki, Osaka 569-8686, Japan[3]; and Department of Immunology, Graduate School of Medicine, University of the Ryukyus, Nishihara, Okinawa 903-0215, Japan[4]

Received 14 May 2007/Accepted 27 October 2007

Accumulating evidence indicates that human immunodeficiency virus type 1 (HIV-1) acquires various cellular membrane proteins in the lipid bilayer of the viral envelope membrane. Although some virion-incorporated cellular membrane proteins are known to potently affect HIV-1 infectivity, the virological functions of most virion-incorporated membrane proteins remain unclear. Among these host proteins, we found that CD63 was eliminated from the plasma membranes of HIV-1-producing T cells after activation, followed by a decrease in the amount of virion-incorporated CD63, and in contrast, an increase in the infectivity of the released virions. On the other hand, we found that CD63 at the cell surface was preferentially embedded on the membrane of released virions in an HIV-1 envelope protein (Env)-independent manner and that virion-incorporated CD63 had the potential to inhibit HIV-1 Env-mediated infection in a strain-specific manner at the postattachment entry step(s). In addition, these behaviors were commonly observed in other tetraspanin proteins, such as CD9, CD81, CD82, and CD231. However, L6 protein, whose topology is similar to that of tetraspanins but which does not belong to the tetraspanin superfamily, did not have the potential to prevent HIV-1 infection, despite its successful incorporation into the released particles. Taken together, these results suggest that tetraspanin proteins have the unique potential to modulate HIV-1 infectivity through incorporation into released HIV-1 particles, and our findings may provide a clue to undiscovered aspects of HIV-1 entry.

To initiate the infection of human immunodeficiency virus type 1 (HIV-1), the envelope protein (Env) plays a critical role in mediating the attachment of virions to target cells and the following fusion with the cellular membrane (24). HIV-1 Env is composed of the surface protein (gp120) and the transmembrane protein (gp41). gp120 binds first to its primary receptor, CD4 (15, 37), and subsequently to its coreceptor, CXCR4 or CCR5 (10, 17, 19, 20, 22). Thereafter, the ectodomain of gp41 executes fusion of viral envelope and the plasma membrane of target cell (24). Therefore, the incorporation of Env into released virion is a key step in acquiring infectivity.

During the budding process of HIV-1, not only HIV-1 Env but also a variety of cellular membrane proteins are efficiently incorporated into released progeny virions (7), and some of them are involved in HIV-1 infection. For example, HIV-1 infectivity is enhanced by virion-incorporated proteins, such as human leukocyte antigens (HLAs) (6, 13, 44), costimulatory molecules (CD80 and CD86) (21, 25), and intracellular adhesion molecule-1 (ICAM-1) (2, 4). Since their individual counterreceptors are expressed on the surface of HIV-1 target cells, it is thought that the interaction between these membrane proteins on virions and their counterreceptors on target cells facilitates the association of viral particles and the target cells. In addition, virion-incorporated ICAM-1 also has the potential to contribute to virus-to-cell fusion (67). In contrast, it has been shown that CD4 proteins have the potential to prevent HIV-1 infection at the attachment step through incorporation into the released particles (66). Furthermore, there is a report indicating that HIV-1 particles are protected by glycosylphosphatidylinositol-anchored complement control proteins, such as CD55 and CD59, which have the physiological function of preventing the assembly of the membrane attack complex (61). They are inserted into HIV-1 virions and then protect them from complement-mediated viral lysis. However, the virological and immunological functions of most of the other virion-incorporated membrane proteins remain unclear.

CD63 is one of the cellular membrane proteins that are incorporated into HIV-1 virions (9, 46, 55). CD63 is a type II cellular membrane protein and belongs to the tetraspanin superfamily (32, 62). It has been reported that CD63 colocalizes with Gag protein in HIV-1-producing cells (3, 28, 52, 55, 56, 60). In addition, Nydegger et al. showed that CD63 forms tetraspanin-enriched microdomains (TEMs) that collaborate with other tetraspanin proteins, such as CD9, CD81, and CD82, and that TEMs act as the gateway for HIV-1 budding at the plasma membrane (50). Furthermore, Jolly and Sattentau reported that TEM components are accumulated on the sur-

* Corresponding author. Mailing address: Laboratory of Viral Pathogenesis, Institute for Virus Research, Kyoto University, 53 Shogoinkawara-cho, Sakyo-ku, Kyoto, Kyoto 606-8507, Japan. Phone: 81-75-751-4811. Fax: 81-75-751-4812. E-mail: ykoyanag@virus.kyoto-u.ac.jp.

▽ Published ahead of print on 7 November 2007.

faces of HIV-1-producing CD4$^+$ T cells and colocalize with HIV-1 Env and Gag (35).

Recently, it was suggested that CD63 plays roles in HIV-1 replication. For example, Lindern et al. reported that the pretreatment of macrophages with anti-CD63 antibodies inhibits HIV-1 infection (70). In addition, Ho et al. have shown that the recombinant soluble protein of the large extracellular loop (LEL) of CD63 potently inhibits HIV-1 infection to macrophages, presumably at the entry step (33). Nevertheless, the practical role(s) and function(s) of intact CD63 protein in HIV-1 infection are still unclear.

Here, we investigated whether CD63 has any virological function in HIV-1 infection. We observed that CD63 was removed from the plasma membrane of HIV-1-producing T cells by activation stimuli, and that the activated cells released HIV-1 virions that contained smaller amounts of CD63 and had higher infectivity. In addition, through exogenous expression experiments, we found evidence suggesting that CD63 at the plasma membrane of HIV-1-producing cells was efficiently incorporated into released virions and that virion-incorporated CD63 had the potential to impair HIV-1 Env-mediated infection in a strain-specific manner at the postattachment step(s). Similar behavior was also observed in other tetraspanin proteins, such as CD9, CD81, CD82, and CD231. However, L6, which has topology similar to that of tetraspanins but does not belong to the tetraspanin superfamily, did not have the potential to prevent HIV-1 infection. These are the first findings suggesting that some cellular membrane proteins can attenuate HIV-1 Env-mediated infection in a strain-specific manner through incorporation into released HIV-1 particles.

MATERIALS AND METHODS

Cells. 293T cells and MAGIC-5 cells (HeLa cells transduced with genes for CD4, CCR5, and long terminal repeat-driving β-galactosidase) (29) were maintained in Dulbecco's modified Eagle medium containing 10% fetal calf serum (FCS), 100 U/ml penicillin, and 100 μg/ml streptomycin. Molt4/IIIB cells, which persistently produce HIV-1_{IIIB} (39), and MT-4 cells were maintained in RPMI 1640 medium containing 10% FCS, 100 U/ml penicillin, and 100 μg/ml streptomycin. To activate Molt4/IIIB cells, 1 μg/ml phytohemagglutinin (PHA) and 100 ng/ml phorbol 12-myristate 13-acetate (PMA) were added, and cells were cultured for 72 h. To prepare activated primary CD4$^+$ T cells, peripheral blood mononuclear cells (PBMCs) were isolated from peripheral blood of healthy HIV-1-seronegative donors as previously described (41). CD4$^+$ T cells were isolated from the PBMCs by using a CD4-positive-cell isolation kit (Dynal, Oslo, Norway) and were activated by using a Dynabeads CD3/CD28 T-cell expander (Dynal) according to the manufacturer's instructions. Activated primary CD4$^+$ T cells were maintained in RPMI 1640 containing 10% FCS, 100 U/ml interleukin-2 (Shionogi, Osaka, Japan), 100 U/ml penicillin, and 100 μg/ml streptomycin.

Plasmid construction. To construct a CD63 expression plasmid (pCD63), a *cd63* cDNA fragment was amplified by PCR from a human leukocyte cDNA library (Invitrogen, Carlsbad, CA) using the following primers: sense, 5′-TA GCG AAT TCC ATG GCG GTG GAA GGA G-3′; antisense, 5′-TA GCT CTA GAC CTA CAT CAC CTC GTA GCC ACT-3′. The resulting fragment was digested with EcoRI and XbaI and inserted into the EcoRI-XbaI site of pCMV-SPORT6 (Invitrogen). To construct CD9-, CD81-, CD82-, and CD231-expressing plasmids (pCD9, pCD81, pCD82, and pCD231), *cd9*, *cd81*, *cd82*, and *cd231* cDNA fragments were obtained similarly, using the following primers: *cd9* sense, 5′-TT TTG AAT TCC ATG CCG GTC AAA GGA GGC A-3′; *cd9* antisense, 5′-TT TTT GAT ATC CTA GAC CAT CTC GCG GTT CCT-3′; *cd81* sense, 5′-TT TTG AAT TCC ATG GGA GTG GAG GGC TGC A-3′; *cd81* antisense, 5′-TT TTT GAT ATC TCA GTA CAC GGA GCT GTT CCG GAT-3′; *cd82* sense, 5′-TT TTG AAT TCC ATG GGC TCA GCC TGT ATC AAA G-3′; *cd82* antisense, 5′-TT TTT GAT ATC TCA GTA CTT GGG GAC CTT GCT GT A-3′; *cd231* sense, 5′-TT TTG GTA CCC ATG GCA TCG AGG AGA ATG GA-3′; *cd231* antisense, 5′-TT TTT GAT ATC TTA CAC CAT CTC ATA CTG ATT GGC-3′. The *cd9* cDNA fragment was also amplified from the leukocyte library, whereas *cd81*, *cd82*, and *cd231* cDNA fragments were obtained by reverse transcription-PCR of mRNA derived from Jurkat cells. These cDNA fragments were digested with EcoRI and EcoRV and inserted into the EcoRI-EcoRV site of pCMV-SPORT6. To construct an L6-expressing plasmid (pL6), *l6* cDNA was obtained from pRcCMV-L6 (kindly provided by E. Mekada) using the following primers: *l6* sense, 5′-TT TTG GTA CCC ATG TGC TAT GGG AAG TGT GCA-3′; *l6* antisense, 5′-TT TTT GAT ATC TTA GCA GTC ATA TTG CTG TTG GTG-3′. The resulting fragment was digested with KpnI and EcoRI and inserted into the KpnI-EcoRI site of pCMV-SPORT6. To construct pCD63ΔL, expressing a CD63 with the lysosomal sorting motif deleted (CD63ΔL), pCD63 was digested with PstI and XbaI, and the following mutagenic oligonucleotides were inserted: sense, 5′-GCA GCC CTT GGA ATT GCT TTT GTC GAG GTT TTG GGA ATT GTC TTT GCC TGC TGC CTC GTG AAG AGT ATC AGA TAG T-3′; antisense, 5′-CT AGA CTA TCT GAT ACT CTT CAC GAG GCA GCA GGC AAA GAC AAT TCC CAA AAC CTC GAC AAA AGC AAT TCC AAG GGC TGC TGC A-3′. To construct pJRFLenv, a HindIII-XhoI fragment containing HIV-$1_{JR\text{-}FL}$ *tat*, *rev*, and *env* was inserted into pGEM4 (Promega, Madison, WI). To construct pNL4-3Δenv (which lacks HIV-$1_{NL4\text{-}3}$ *env*), pNL4-3 was digested with NheI, blunted, and self-ligated. PCR was carried out with the Expand Long Template PCR system (Roche, Mannheim, Germany), and reverse transcription-PCR was carried out by using SuperScript One-Step RT-PCR with Platinum high-fidelity *Taq* (Invitrogen), according to the manufacturer's protocols. Sequences of these plasmid constructs were confirmed with an ABI Prism 3100 genetic analyzer (Applied Biosystems, Foster City, CA).

Virus preparation. 293T cells were seeded to appropriate densities 1 day prior to transfection and were transfected by the calcium phosphate method as described previously (36). The culture supernatants were harvested, centrifuged, and then filtrated to produce virus solutions at 48 h posttransfection. To prepare HIV-1 and virus-like particles (VLPs), cells were cotransfected with pNL4-3 (1), pJR-FL (40), pNLFLV3 (kindly provided by W. A. O'Brien) (63), pNL4-3Δenv, and either tetraspanin-expressing plasmids or pCMV-SPORT6 (empty vector). To prepare pseudotyped viruses with envelope protein (Env) from either HIV-1 (NL4-3, IIIB, JR-FL, and NL4-3ΔCT, which encodes an NL4-3 Env with a deletion of the cytoplasmic tail [CT]) or vesicular stomatitis virus (VSV), cells were cotransfected with the Env expression plasmid DNA, pIIINL4env (kindly donated by T. Murakami and E. O. Freed) (48), pLET (59), pJRFLenv, pIIINL4envCTdel-144-2 (kindly donated by T. Murakami and E. O. Freed) (48), or pMD.G (53), respectively, and with pNLLuc (an Env-defective HIV-$1_{NL4\text{-}3}$ carrying the luciferase gene) (57) and either tetraspanin-expressing plasmids or empty vector. To prepare β-lactamase (BlaM)-conjugated Vpr-containing NL4-3 (NL4-$3^{BlaM\text{-}Vpr}$), pNL4-3 and pCMV4-3BlaM-Vpr (kindly provided by W. C. Greene) (8) were cotransfected with pCD63 or empty vector. To prepare HIV-1_{IIIB}, culture supernatants of Molt4/IIIB cells were harvested, centrifuged, and then filtered to produce virus solutions.

Antibodies and reagents. The following antibodies and reagents were used in this study: anti-CD63 mouse monoclonal antibody (mMAb) (MX-49.129.5; Santa Cruz Biotechnology, Santa Cruz, CA); anti-CD9 mMAb (M-L13; BD Biosciences, San Jose, CA); anti-CD81 mMAb (1D6; Serotec, Oxford, United Kingdom); anti-CD82 mMAb (B-L2; Serotec); anti-CD231 mMAb (H1-A12; BD Biosciences); anti-L6 mMAb (D1-D2; Chemicon, Temecula, CA); anti-CD45 mMAb (H130; BD Biosciences); anti-β-actin mMAb (AC-15; Sigma, St. Louis, MO); rat anti-gp120 MAb (W#10, which recognizes the V3 region of HIV_{IIIB} Env [Y. Tanaka, unpublished data]); goat anti-$p24^{CA}$ antiserum (ViroStat, Portland, ME); anti-$p17^{MA}$ mMAb (Applied Biotechnologies, Columbia, MD), which recognizes $p17^{MA}$ but not $Pr55^{Gag}$ (51); anti-Vpr mMAb (8D1; kindly donated by Y. Ishizaka); biotinylated horse anti-mouse immunoglobulin G (IgG) Ab (Vector Laboratories, Burlingame, CA); biotinylated donkey anti-rat IgG Ab (Rockland, Gilbertsville, PA); biotinylated donkey anti-goat IgG Ab (Chemicon); biotinylated donkey anti-rabbit IgG Ab (Chemicon); horseradish peroxidase-conjugated horse anti-mouse IgG Ab (Cell Signaling, Denver, MA); horseradish peroxidase-conjugated streptavidin (SA; Zymed, San Francisco, CA); and Alexa Fluor 488-conjugated goat anti-mouse IgG Ab (Molecular Probes, Eugene, OR).

Flow cytometry. In brief, cells were suspended in phosphate-buffered saline (PBS) and incubated for 30 min with appropriate antibodies at 4°C. Flow cytometry was performed with a FACScan (BD Biosciences), and data were analyzed using CellQuest software (BD Biosciences).

Immunoelectron microscopy. Cells were fixed with 0.2% glutaraldehyde in 150 mM PBS (pH 7.2) for 3 min at room temperature and harvested. The collected cells were fixed again with 1% glutaraldehyde in 150 mM PBS at 4°C for 60 min, dehydrated in a graded ethanol series, and embedded in Lowicryl K4M resin. Ultrathin sections were prepared using an ultramicrotome Reichert-Nissei Ul-

tracut-N (Leica, Vienna, Austria), and mounted on a nickel grid supported by a carbon-coated collodion film. The sections on the grid were treated with 5% goat serum in 150 mM PBS (pH 7.2) to block nonspecific reactions. The sections were treated with anti-CD63 mMAb at room temperature for 180 min. After washing three times, the sections were treated with goat serum containing 5-nm colloidal gold-labeled anti-mouse IgG (Amersham, Little Chalfont, United Kingdom) at room temperature for 60 min and washed in PBS. The immunostained sections were fixed with 1% glutaraldehyde in 50 mM cacodylate buffer again and washed in distilled water. The immunolabeled sections were treated with a mixture of 0.01% ruthenium red and 0.5% osmium tetroxide in 50 mM cacodylate buffer at room temperature for 10 min and double stained with uranyl acetate for 20 min, as previously described (38). The sections were observed under an electron microscope (H-7650; Hitachi, Ibaraki, Japan).

Western blotting and slot blotting. Cells were lysed with lysis buffer (1% Triton X-100, 50 mM Tris-HCl [pH 8.0], 150 mM NaCl, and protease inhibitor complete cocktail [Roche]). Virions were concentrated by ultracentrifugation at 100,000 × *g* for 1 h at 4°C, and pellets were lysed with lysis buffer. For Western blotting, lysates were separated by sodium dodecyl sulfate-polyacrylamide gel electrophoresis and transferred to Immobilon transfer membranes (Millipore, Bedford, MA). For detection, appropriate antibodies were used. Slot blotting was performed with a Hybri-slot Manifold (Invitrogen), according to the manufacturer's instructions.

Virus titration. IIIB was titrated by 50% tissue culture infective dose ($TCID_{50}$), and the infectious units (IU) of NL4-3, JR-FL, and NLFLV3 were measured by Magi assay, as follows.

(i) $TCID_{50}$. Virus solutions (HIV-1_{IIIB}) were serially diluted with RPMI 1640, and each solution was inoculated onto 6×10^4 MT-4 cells in quadruplicate. The $TCID_{50}$ was calculated as previously described (31).

(ii) Magi assay. MAGIC-5 cells (3×10^4) were seeded into a 24-well plate, 24 h before infection. Virus solutions (HIV-1_{NL4-3}, HIV-1_{JR-FL}, and HIV-1_{NLFLV3}) were diluted appropriately, 200 μl of the solutions was inoculated onto MAGIC-5 cells, and cells were incubated for 2 h at 37°C in a CO_2 incubator. After infection, 1 ml of conditioned medium was added for quenching, and the culture was further incubated for 48 h under the same conditions. Cells were fixed in fixing solution (1% formaldehyde, 0.2% glutaraldehyde in PBS) at 48 h postinfection and then treated with staining solution (400 μg/ml X-Gal [5-bromo-4-chloro-3-indolyl-β-D-galactopyranoside], 4 mM potassium ferrocyanide, 4 mM potassium ferricyanide, 2 mM $MgCl_2$ in PBS). Blue-stained cells in each well were counted in five fields, and the IU were calculated as previously described (29).

ELISA. To quantify $p24^{CA}$ in virus solutions, an HIV-1 p24 antigen enzyme-linked immunosorbent assay (ELISA) kit (ZetroMetrix, Buffalo, NY) was used according to the manufacturer's instructions.

Virus precipitation assay. Virus immunoprecipitation was performed as described previously (21), with some modifications. In brief, virus solution (100 ng of $p24^{CA}$) in PBS containing 3% bovine serum albumin (BSA) was incubated with 1 μg of each Ab overnight at 4°C. To harvest the virus-Ab complex, 25 μl of Dynabeads protein G (Dynal) in 3% BSA in PBS was added, and the mixture was held for 30 min at room temperature. The captured viruses were then precipitated with a magnet, washed with 3% BSA in PBS, and lysed with lysis buffer. $p24^{CA}$ was quantified by ELISA, as described above, and the amount of bound virions was calculated.

Pseudotyped virus infection and luciferase assay. To measure the infectivity of NL4-3 Env, IIIB Env, and NL4-3ΔCT Env-pseudotyped virus, MAGIC-5 cells (2×10^5) or MT-4 cells (1.5×10^5) were incubated for 48 h in an aliquot of each virus solution, containing 5 ng or 0.5 ng of $p24^{CA}$. A solution of JR-FL Env-pseudotyped virus, containing 20 ng of $p24^{CA}$, was incubated with MAGIC-5 cells (1×10^5) for 72 h. A solution of VSV envelope glycoprotein (VSV-G)-pseudotyped virus, containing 0.5 ng of $p24^{CA}$, was incubated with both MAGIC-5 cells (2×10^5) and MT-4 cells (1.5×10^5) for 48 h. Activated primary $CD4^+$ T cells (1×10^6) were inoculated with NL4-3 Env-pseudotyped virus, containing 10 ng of $p24^{CA}$, and incubated for 48 h. The Picagene luciferase assay kit (Toyo Ink, Tokyo, Japan) was used to perform luciferase assays, following the manufacturer's protocols. Activity was measured with a 1420 ARVOSX multilabel counter (Perkin Elmer, Wellesley, MA) and normalized to the protein content of each lysate, measured with a Coomassie (Bradford) protein assay kit (Pierce, Rockford, IL). All experiments were performed in triplicate.

Virus attachment assay. The virus attachment assay was performed as described previously (66) with some modifications. In brief, MT-4 cells (2×10^5) were incubated for 2 h at 4°C with an aliquot of HIV-1 containing 10 ng of $p24^{CA}$. After the incubation, cells were washed once with chilled Dulbecco's modified Eagle medium and five times with chilled PBS before being lysed with lysis buffer. The amounts of $p24^{CA}$ in these lysates were determined by ELISA, as described above, and the amount of attached virions was calculated.

HIV-1 fusion assay. The HIV-1 fusion assay, which is based on the incorporation of β-lactamase–Vpr chimeric proteins (BlaM-Vpr) into virions and subsequent BlaM cleavage of a fluorescent dye (CCF2) present in target cells, was performed as described previously (8). In brief, MT-4 cells (5×10^5) were incubated for 3 h at 37°C in a CO_2 incubator, with aliquots of NL4-$3^{BlaM-Vpr}$ containing 100 ng of $p24^{CA}$. Cells were washed once with an equilibrated buffer (RPMI 1640 containing 10% FCS and 20 mM HEPES-NaOH [pH 7.4]) and then incubated in 100 μl of substrate loading buffer (2 μM CCF2-AM in the equilibrated buffer, prepared according to the manufacturer's instructions [Invitrogen]) for 1 h at room temperature. After washing twice with the equilibrated buffer, cells were incubated in an equilibrated buffer containing 2.5 mM probenecid (Sigma) for 7 h at room temperature, to allow the BlaM reaction to develop. Finally, cells were washed once with PBS and fixed in 1% formalin neutral buffer solution. The change in emission fluorescence of the CCF2 dye, following its cleavage by BlaM-Vpr, was monitored by flow cytometry with FACSAria (BD Biosciences). Data were analyzed with FACSDiva software (BD Biosciences) and evaluated as previously described (8).

Real-time PCR. The amount of HIV-1 reverse transcripts (RT) was determined as previously described (64). In brief, to completely remove contaminating transfected pNL4-3 plasmid DNA, the virus solution was preincubated with DNase I (3,500 U/ml; Takara Bio, Shiga, Japan) containing 10 mM $MgCl_2$ for 30 min at room temperature. MT-4 cells (4×10^5) were incubated for 2 h at 37°C with aliquots of HIV-1 containing 2 ng of $p24^{CA}$. After infection, the cells were vigorously washed and cultured for 3 or 6 h. DNA was extracted by the urea-lysis method, and 500 ng of DNA was used as the template. Real-time PCR was performed by using a 7500 real-time system (Applied Biosystems), and data were analyzed with 7500 system SDS software (Applied Biosystems) and evaluated as previously described (64).

Statistical analysis. Student's *t* test was used to determine statistical significance. *P* values of <0.05, <0.01, and <0.001 were considered significant.

RESULTS

Activation of Molt4/IIIB cells intensifies HIV-1 infectivity and eliminates CD63 from both the released virions and the plasma membrane. The activation stimulus causes augmentation of HIV-1 production (30, 74). We stimulated Molt4/IIIB cells, which persistently produce infectious HIV-1_{IIIB} virions (39), with PHA and PMA and detected a threefold increase in the amount of $p24^{CA}$ released into the culture supernatant, as measured by ELISA (Fig. 1A). Interestingly, we also found that PHA/PMA activation significantly enhanced the infectivity of released HIV-1_{IIIB} virions (Fig. 1B). We first suspected that it might have been caused by the increase in the amount of mature HIV-1 Env, gp120, incorporated into HIV-1 particles. However, as shown in Fig. 1C, there was little change in the amount of gp120. Instead, the virus precipitation assay (21) revealed a large reduction in the virion-incorporated CD63 (Fig. 1D). As one of negative controls for this assay, we used an anti-CD45 antibody. It has already been proven that CD45 is expressed on the plasma membrane of leukocytes but is hardly incorporated into HIV-1 particles (49, 69). As previously reported, this antibody did not capture HIV-1 particles (Fig. 1D), suggesting that our assay specifically captured CD63 protein on the released HIV-1 particles. Correspondingly, we observed that CD63 expression on the surface of Molt4/IIIB cells was significantly down-modulated following PHA/PMA activation (Fig. 1E and F). As we suspected that the decrease of CD63 on virus particles might be related to the enhancement of virus infectivity, in subsequent experiments, we investigated the role of CD63 in the modulation of HIV-1 infectivity.

CD63 is incorporated into virions in an Env-independent manner and reduces infectivity. To directly examine the po-

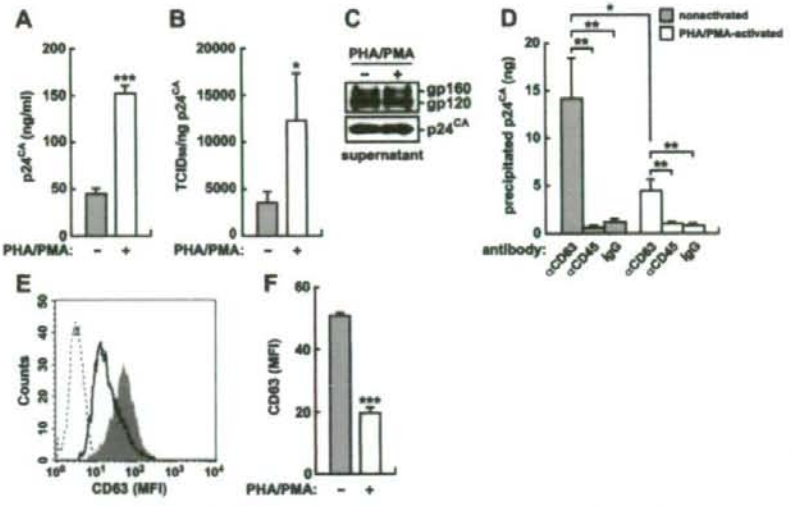

FIG. 1. Inverse correlation between HIV-1 infectivity and the level of CD63 in the released virions. Molt4/IIIB cells were activated with PHA (1 μg/ml) and PMA (100 ng/ml) for 72 h. (A) HIV-1_{IIIB} particles released from nonactivated or PHA/PMA-activated Molt4/IIIB cells were quantitated by $p24^{CA}$ ELISA. (B) The $TCID_{50}$ was measured as described in Materials and Methods and was normalized to the amount to $p24^{CA}$. (C) The level of Env in HIV-1_{IIIB} particles was analyzed by Western blotting. The input was standardized to $p24^{CA}$, and a representative result is shown. (D) The virus precipitation assay was performed as described in Materials and Methods. HIV-1_{IIIB} particles (100 ng of $p24^{CA}$) released from nonactivated or PHA/PMA-activated Molt4/IIIB cells were used for immunoprecipitation by respective antibodies. (E and F) The surface expression of CD63 on nonactivated (filled in gray) and PHA/PMA-activated (black line) Molt4/IIIB cells was analyzed by flow cytometry. Isotype IgG was used as a negative control (broken line). A representative result is shown in panel E, and summarized results are shown in panel F. Experiments were performed in triplicate. Statistical significance (Student's *t* test) is shown as follows: *, $P < 0.05$; **, $P < 0.01$; ***, $P < 0.001$. Error bars indicate standard deviations. MFI, mean fluorescence intensity.

tential of virion-incorporated CD63, we cotransfected a CD63 expression plasmid (pCD63) and pNL4-3 into 293T cells. Western blotting analyses showed that exogenous expression of CD63 did not influence the expression of HIV-1 components (Fig. 2A, top) and that there was little change in either the amount of released HIV-1 particles (Fig. 2C) or the detected HIV-1 components, including Env (gp120 and gp160), Gag (precursor protein [$Pr55^{Gag}$], cleavage intermediate [$p41^{MA-CA}$], $p24^{CA}$, and $p17^{MA}$), and Vpr (Fig. 2A, bottom). In addition, pNL4-3 transfection did not affect the surface expression of CD63, and exogenous CD63 was successfully expressed on the surfaces of 293T cells (Fig. 2B). In the virus precipitation assay, we observed that the level of endogenous CD63 on conventional HIV-1_{NL4-3} particles (Fig. 2D) was similar to that on HIV-1_{IIIB} particles released from PHA/PMA-activated Molt4/IIIB cells (Fig. 1D). Likewise, exogenous CD63 was efficiently incorporated into the released HIV-1_{NL4-3} (Fig. 2D) in amounts comparable to those in HIV-1_{IIIB} released from nonactivated Molt4/IIIB cells (Fig. 1D). These observations suggest that this 293T cell system may be an appropriate system for studying the phenomenon in Molt4/IIIB cells. Moreover, immunoelectron microscopy with an anti-CD63 antibody confirmed the presence of endogenous CD63 in HIV-1 particles (Fig. 2F), and the amount of virion-incorporated CD63 was increased by the exogenous expression (Fig. 2G). To analyze the necessity of Env for incorporation CD63 into released virions, we cotransfected cells with pCD63 and pNL4-3Δenv, which lacks NL4-3 *env* and produces virus-like particles. As shown in Fig. 2E, the level of CD63 on virus-like particles was comparable to that in wild-type NL4-3. Because ICAM-1 and HLA-DR are incorporated into released HIV-1 particles in an Env-independent manner (2, 44), it would not be surprising to find that Env is dispensable for the incorporation of CD63 into the released HIV-1 virions.

To investigate the virions released from pCD63-transfected cells further, we measured infectivity with a Magi assay (29). Although $p24^{CA}$ ELISA indicated that the amounts of released virions were comparable (Fig. 2C), the Magi assay revealed that the virions released from pCD63-transfected cells were significantly less infectious than typical virions (Fig. 2H). These results suggest that CD63 proteins on HIV-1 particles may have a suppressive effect on HIV-1 infection.

Non-virion-associated CD63 has no effect on HIV-1 infection. As shown in Fig. 2A, we observed that CD63 proteins are also released from the cells transfected solely with pCD63. It was recently reported that recombinant large extracellular domains of tetraspanin proteins, including CD63, potently inhibit HIV-1 infection (33). To eliminate the possibility that the infectivity reduction was caused by non-virion-associated CD63, we pretreated HIV-1 particles or target cells with the culture supernatant of the cells transfected solely with pCD63 (Fig. 3A) and evaluated the effect on HIV-1 infectivity by Magi assay. However, non-virion-associated CD63 did not affect HIV-1 infectivity (Fig. 3B to D). Moreover, we also examined whether non-virion-associated CD63 interferes with the virus precipitation assay. As shown in Fig. 3E, however, non-virion-associated CD63 did not affect virus precipitation by anti-

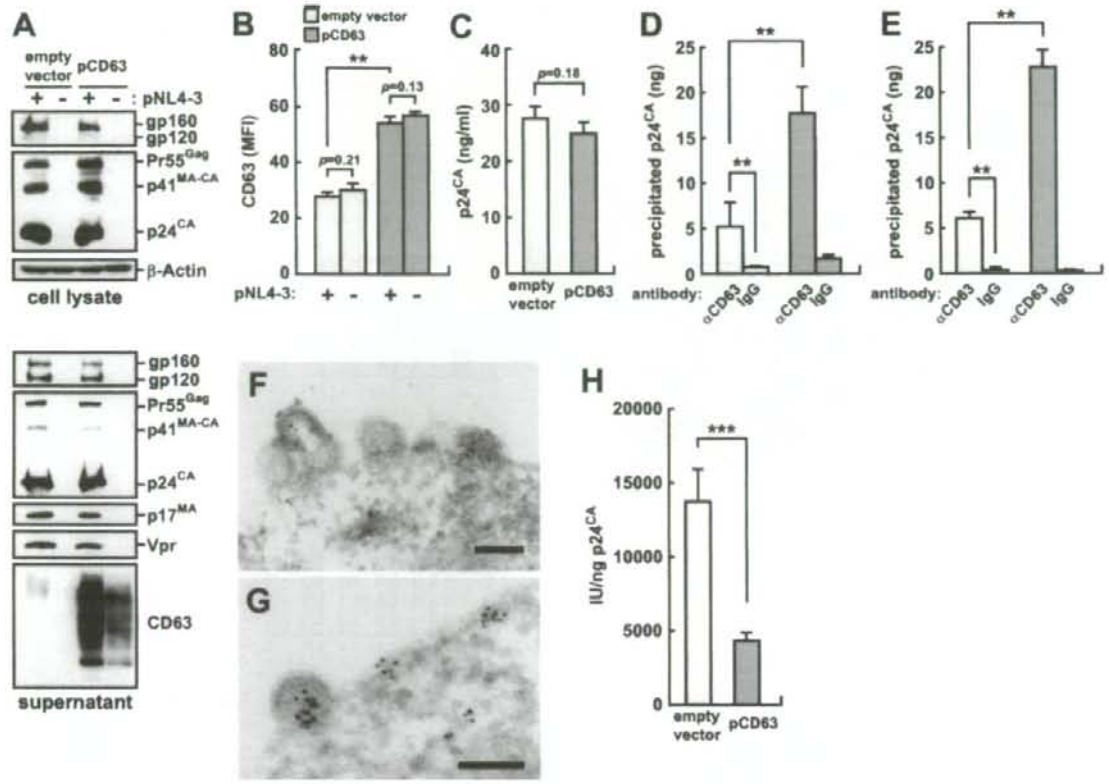

FIG. 2. Incorporation of exogenous CD63 into released HIV-1 virions and suppression of infectivity. Plasmid DNAs (pNL4-3 and either pCD63 or empty vector) were cotransfected into 293T cells as described in Materials and Methods. (A) Viral protein expression in the transfected 293T cells (cell lysate) and viral components in released HIV-1_{NL4-3} particles (supernatant) were analyzed by Western blotting, and a representative result is shown. The cell number was normalized to β-actin, and the released virions were harvested as described in Materials and Methods. (B) The surface expression of CD63 on empty vector-cotransfected and pCD63-cotransfected 293T cells was analyzed by flow cytometry. (C) The amount of released HIV-1_{NL4-3} particles released from empty vector-cotransfected or pCD63-cotransfected 293T cells was quantitated by $p24^{CA}$ ELISA. (D and E) HIV-1_{NL4-3} particles (D) and virus-like particles (E) (100 ng of $p24^{CA}$) released from empty vector-cotransfected or pCD63-cotransfected 293T cells were used for immunoprecipitation by respective antibodies, and the assay was performed as described in Materials and Methods. (F and G) Immunoelectron microscopy was performed as described in Materials and Methods. CD63 on HIV-1_{NL4-3} particles released from empty vector-cotransfected (F) and pCD63-cotransfected (G) 293T cells was detected by using anti-CD63 mouse antibody and was visualized with anti-mouse IgG 5-nm gold colloid (black dots). Bars, 100 nm. (H) IU of HIV-1_{NL4-3} released from empty vector-cotransfected or pCD63-cotransfected 293T cells were measured by Magi assay and were normalized to $p24^{CA}$. Experiments were performed in triplicate. Statistical significance (Student's t test) is shown as follows: **, $P < 0.01$; ***, $P < 0.001$. Error bars indicate standard deviations. MFI, mean fluorescence intensity.

CD63 antibody. In summary, the data suggest that only CD63 proteins incorporated into released virions have a role in the attenuation of HIV-1 infectivity.

CD63 on the cell surface is preferentially incorporated into the released virions. To investigate the correlation between HIV-1 infectivity and the level of CD63 on the released virions and on the surfaces of HIV-1-producing cells, we prepared pCD63ΔL, expressing a lysosomal target motif-deleted CD63. In agreement with a previous report (34), CD63ΔL was present in larger quantities on the cell surface than wild-type CD63 was (Fig. 4B), although the total amount of expressed protein was comparable to that of wild-type CD63 (Fig. 4A, top).

Using this plasmid, we investigated the effect of CD63ΔL on the infectivity of released virions. Although CD63ΔL did not affect the amount of either $p24^{CA}$ or gp120 released into the culture supernatant (Fig. 4A and C), it severely attenuated the infectivity of released NL4-3 (Fig. 4D). Furthermore, we noticed that CD63ΔL was incorporated into released virions in larger amounts than wild-type CD63 (Fig. 4E). These results suggest that infectivity is inversely correlated with the amount of CD63 (CD63ΔL) on both the released virions and the plasma membranes of HIV-1-producing cells.

Virion-incorporated CD63 impairs NL4-3 Env- and IIIB Env- but not JR-FL Env-mediated infection. To analyze the effect of virion-incorporated CD63 on other HIV-1 strains, we next cotransfected with pJR-FL and pCD63 into 293T cells. As in the case of NL4-3, exogenous CD63 did not affect the amount of released virions and was successfully incorporated

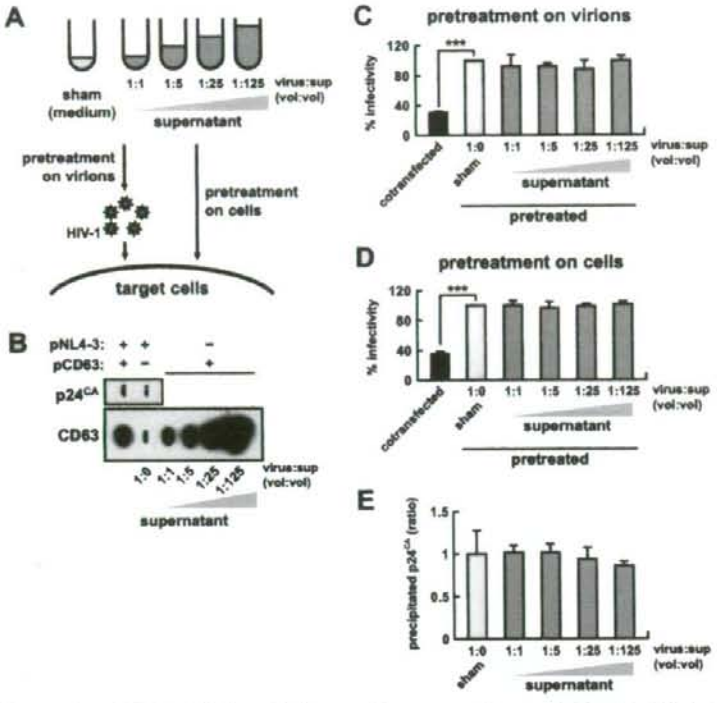

FIG. 3. Effect of non-virion-associated CD63. (A) Schematic diagram of the assay used for panels C and D. (B) Slot blotting shows the relative amounts of CD63 in each culture supernatant used for treatment. (C and D) Non-virion-associated CD63 was used to pretreat virions (C) or target cells (D), and the effect was assessed by Magi assay. RPMI 1640 was used as negative controls (sham), and the infectivity in controls was defined as 100%. The black bars indicate the infectivity of the virions released from the 293T cells cotransfected with pNL4-3 and pCD63, used as positive controls. (E) Effect of non-virion-associated CD63 in a virus precipitation assay. The amount of precipitated virions was quantified as described in Materials and Methods, and the ratio of amounts of precipitated virions to the sham-pretreated control was shown. The relative volumes of the supernatant shown schematically (A) and quantitatively (B) are identical to those used for panels C to E. Experiments were performed in triplicate. The *P* value versus sham-pretreated controls is <0.001 by Student's *t* test (***). Error bars indicate standard deviations.

into the released JR-FL (data not shown). However, virion-incorporated CD63 did not attenuate the infectivity of JR-FL (Fig. 5B).

NL4-3 uses CXCR4 as its coreceptor, whereas JR-FL uses CCR5, and coreceptor usage is severely dependent on the V3 region of Env (11). To investigate the possibility that the function of virion-incorporated CD63 is dependent on coreceptor usage, we used a chimeric HIV-1, NLFLV3. Although NLFLV3 uses CCR5 as its coreceptor (Fig. 5A) (18, 63), the infectivity of NLFLV3 was suppressed in a manner similar to that of wild-type NL4-3 (Fig. 5B). This result indicates that CD63 has the potential to reduce the infectivity of HIV-1 virions in a strain-specific manner and that it does not depend on coreceptor usage.

By cotransfecting pCD63 and pNLLuc, which has a defect in *env* and contains the luciferase gene (*luc*) in NL4-3 DNA, with Env (NL4-3 Env, IIIB Env, a CT-deleted NL4-3 [NL4-3ΔCT] Env, JR-FL Env, or VSV-G) expression plasmids, we prepared various pseudotyped viruses that each have Env on the *luc*-carrying particles. We observed that virion-incorporated CD63 suppressed the infectivity of viruses pseudotyped with NL4-3 Env (Fig. 6A) and IIIB Env (Fig. 6B) in a dose-dependent manner but did not affect that of viruses pseudotyped with JR-FL Env (Fig. 6D) and VSV-G (Fig. 6E). In addition, we found that the infectivity of viruses pseudotyped with NL4-3ΔCT Env was also attenuated through exogenous CD63 (Fig. 6C). Although it has been reported that the impediment of the association between Env CT and $p17^{MA}$ leads to repression of HIV-1 infection (16, 73), this result indicates that virion-incorporated CD63 does not affect the association of Env CT and $p17^{MA}$ at the lining of the viral membrane. Since the pseudotyped viruses differ only in Env, these results indicate that the effect of virion-incorporated CD63 is determined by Env. Moreover, the reduction in infectivity was also confirmed in activated primary $CD4^+$ T cells (Fig. 6F).

Virion-incorporated CD63 inhibits HIV-1 infection at the postattachment entry step(s). The process of HIV-1 entry into target cells has been extensively studied (23). The results described above indicate that virion-incorporated CD63 has the potential to disrupt NL4-3 and IIIB Env-mediated virus entry, and the disruption can negatively influence either attachment to CD4 on target cells or a conformational change of Env leading to virus-to-cell fusion mediated by gp41.

To address these possibilities, we initially compared the

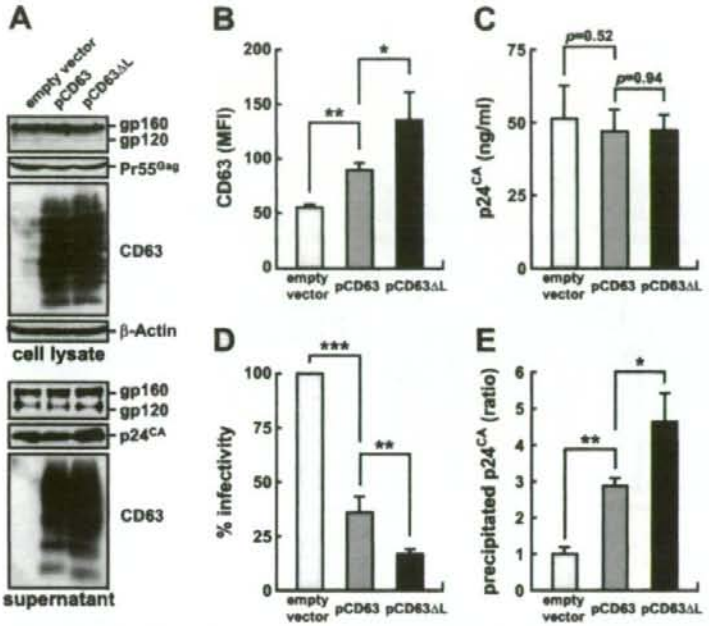

FIG. 4. Augmented reduction of the infectivity of released HIV-1 virions by CD63ΔL. Empty vector, pCD63, and pCD63ΔL were each cotransfected with pNL4-3 into 293T cells. (A) The expression of viral protein and CD63 in the transfected 293T cells and the components of released HIV-1_{NL4-3} particles were analyzed by Western blotting, and a representative result is shown. The cell number was normalized in comparison with β-actin, and the released virions were harvested as described in Materials and Methods. (B) The surface expression of CD63 on the transfected 293T cells was analyzed by flow cytometry. (C) The amount of released HIV-1_{NL4-3} particles was quantitated by $p24^{CA}$ ELISA. (D) IU of HIV-1_{NL4-3} was measured by Magi assay. The IU were normalized to the amount of $p24^{CA}$, and infectivity is shown as a percentage of the empty-vector value. (E) HIV-1_{NL4-3} particles (100 ng of $p24^{CA}$) were used for immunoprecipitation by anti-CD63 antibody. The ratio of precipitated virions to empty vector is shown. Experiments were performed in triplicate. Statistical significance (Student's *t* test) is shown as follows: *, $P < 0.05$; **, $P < 0.01$; ***, $P < 0.001$. Error bars indicate standard deviations. MFI, mean fluorescence intensity.

binding affinity of conventional and CD63-enriched virions. As shown in Fig. 7A, the binding affinity of CD63-enriched virions was not attenuated. To investigate the effect of CD63 on the HIV-1 fusion, we employed an enzyme-based HIV-1 fusion assay, involving preparation of BlaM-Vpr-containing virions ($NL4\text{-}3^{BlaM\text{-}Vpr}$), as described previously (8). Exogenous expression of CD63 had no effect on the amount of either virion-incorporated BlaM-Vpr or released virions, and CD63 was also successfully incorporated (data not shown). Using these virions, we studied the fusion of CD63-enriched virions by measuring the enzymatic activity of BlaM, which is taken up into the cytoplasm of target cells as a result of viral fusion. We observed that the uptake of BlaM, which reflects the fusion activity of viruses with target cells, was remarkably reduced in assays using CD63-enriched virions (Fig. 7B). The reduction in fusion efficiency

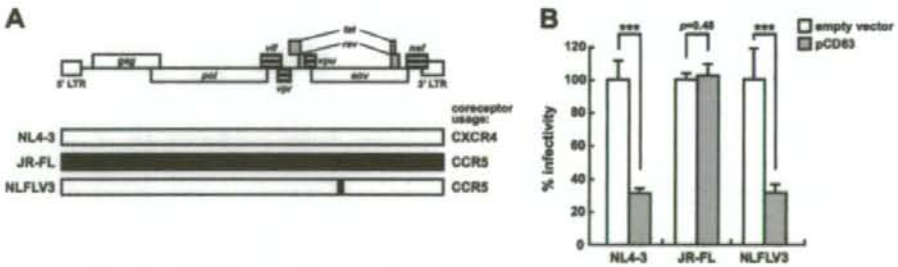

FIG. 5. Effect of virion-incorporated CD63 relative to other HIV-1 strains. (A) HIV-1 strains are schematically shown. (B) IU of respective viruses released from empty vector-cotransfected or pCD63-cotransfected 293T cells were measured by Magi assay. The IU were normalized to the amounts of $p24^{CA}$, and infectivity is shown as a percentage of the empty-vector value. Experiments were performed in triplicate. ***, $P < 0.001$ by Student's *t* test. Error bars indicate standard deviations.

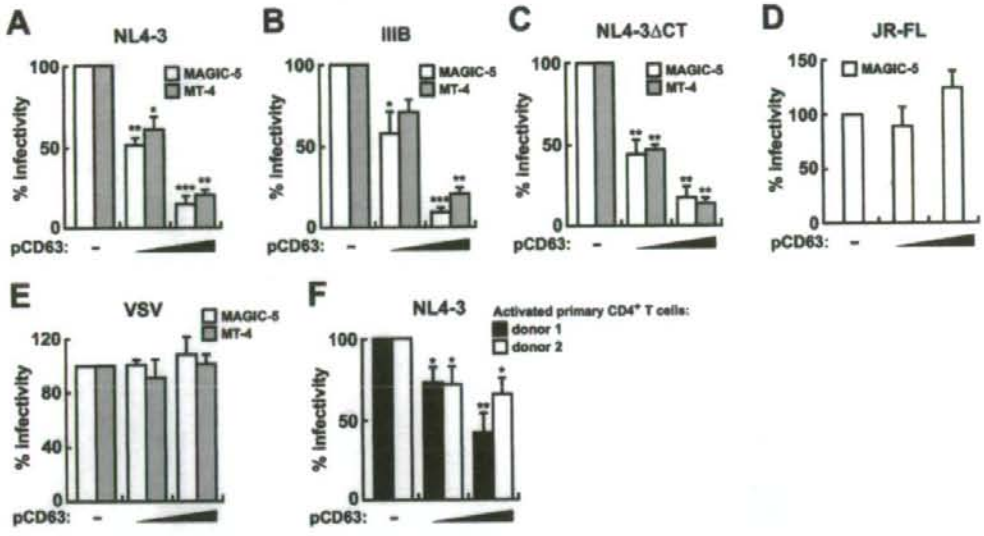

FIG. 6. Pseudotyped virus infection and luciferase assay. The prepared viruses were pseudotyped with Env of NL4-3 (A and F), IIIB (B), NL4-3ΔCT (C), JR-FL (D), or VSV (E). Each pseudotyped virus was prepared by cotransfection with pNLLuc, individual Env expression plasmids, and either empty vector or different doses of pCD63, as described in Materials and Methods. (A to E) MAGIC-5 cells and/or MT-4 cells were used as target cells. (F) NL4-3 Env-pseudotyped viruses were inoculated with CD3/CD28-activated primary $CD4^+$ T cells, and representative results are shown. The average luciferase activities per 1 μg of protein was calculated as relative light units, and infectivity is shown as a percentage of the empty-vector value. Experiments were performed in triplicate. Statistical significance (Student's *t* test) versus empty-vector values is shown as follows: ⋆, $P < 0.05$; ⋆⋆, $P < 0.01$; ⋆⋆⋆; $P < 0.001$. Error bars indicate standard deviations.

corresponded closely to the reduction in infectivity (Fig. 2H). We also quantified HIV-1 RT by real-time PCR. As shown in Fig. 7C and D, both early and late RTs were decreased by CD63 enrichment. We concluded that virion-incorporated CD63 has the potential to prevent a postattachment step mediated by HIV-1 Env leading to the virus-to-cell fusion, and it causes the reduction in infectivity.

Tetraspanin proteins commonly have the potential to suppress HIV-1 infectivity. We analyzed the modulation of cell surface expression of other tetraspanins, CD9, CD81, CD82, and CD231, through cell activation. As shown in Fig. 8A, we observed that surface expression of other tetraspanins on Molt4/IIIB cells was also significantly down-modulated by PHA/PMA activation. Correlating with the surface expression, the amounts of virion-incorporated CD81, CD82, and CD231 were commonly decreased (Fig. 8B), although the amount of virion-incorporated CD9 was not significantly changed because of its lower level of incorporation.

Next, we cotransfected cells with pNL4-3 and individual tetraspanin (CD9, CD81, CD82, or CD231) expression plasmids. In addition, as a control protein, we also prepared an L6 expression plasmid. L6 has four transmembrane domains and is topologically similar to tetraspanins but does not belong to the genuine tetraspanin superfamily because of its structural

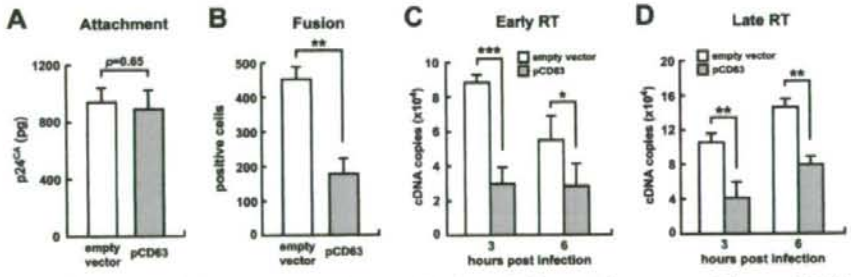

FIG. 7. Effect of virion-incorporated CD63 at early steps of HIV-1 infection. (A) Virus attachment assay. Aliquots of NL4-3 (10 ng of $p24^{CA}$) were incubated with MT-4 cells for 2 h at 4°C. After washing, the cells were lysed, and the amount of bound virions was quantitated by $p24^{CA}$ ELISA. A representative result is shown. (B) Virus fusion assay was performed as described in Materials and Methods, and the number of fused cells in 10,000 cells is shown. (C and D) Real-time PCR was performed as described in Materials and Methods, and the cDNA copy numbers of early (C) and late (D) RT in 100,000 cells are shown. Assays were performed in triplicate. Statistical significance (Student's *t* test) versus empty-vector values is shown as follows: ⋆, $P < 0.05$; ⋆⋆, $P < 0.01$; ⋆⋆⋆, $P < 0.001$. Error bars indicate standard deviations.

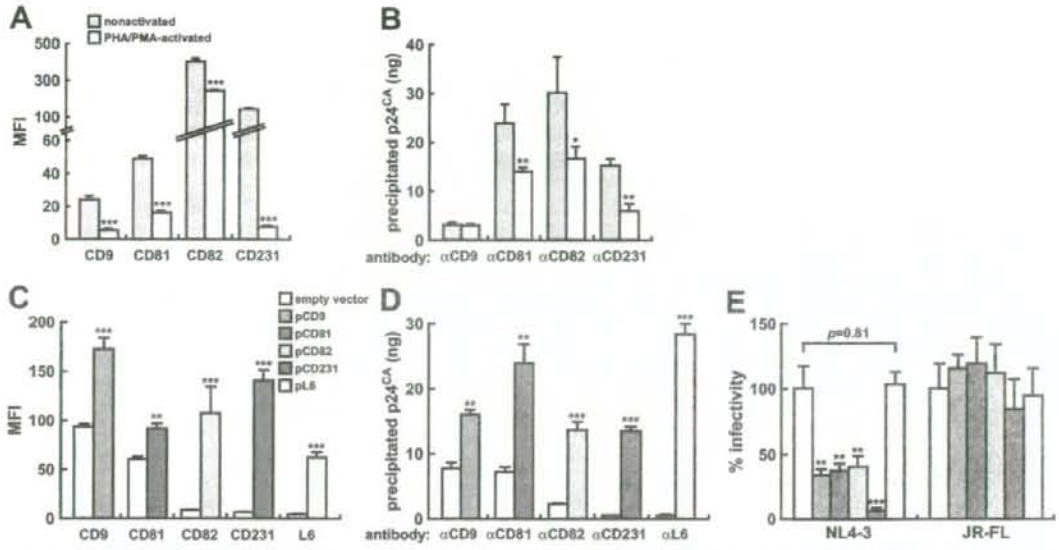

FIG. 8. Correlation between HIV-1 infectivity and the levels of tetraspanins in the released virions. (A and B) Molt4/IIIB cells were activated by PHA and PMA as described for Fig. 1. The surface expression of CD9, CD81, CD82, and CD231 on nonactivated and PHA/PMA-activated Molt4/IIIB cells was analyzed by flow cytometry. (B) The virus precipitation assay was performed as described in Materials and Methods. HIV-1_{IIIB} particles (100 ng of $p24^{CA}$) released from nonactivated or PHA/PMA-activated Molt4/IIIB cells were used for immunoprecipitation by respective antibodies. (C to E) Empty vector or individual tetraspanin-expression plasmids were each cotransfected with pNL4-3 into 293T cells. (C) The surface expression of tetraspanins on the 293T cells cotransfected with pNL4-3 and either empty vector or individual tetraspanin expression plasmids was analyzed by flow cytometry. (D) The virus precipitation assay was performed as described in Materials and Methods. HIV-1_{NL4-3} particles (100 ng of $p24^{CA}$) released from the 293T cells cotransfected with pNL4-3 and either empty vector or individual tetraspanin expression plasmids were used for immunoprecipitation by the respective antibodies. (E) IU of HIV-1_{NL4-3} or HIV-1_{JR-FL} released from the 293T cells cotransfected with pNL4-3 or pJR-FL and either empty vector or individual tetraspanin expression plasmids was measured by Magi assay. The IU were normalized to the amounts of $p24^{CA}$, and infectivity is shown as a percentage of empty-vector values. Experiments were performed in triplicate. Statistical significance compared to nonactivated (A and B) or empty vector (C to E) values (Student's *t* test) is shown as follows: *, $P < 0.05$; **, $P < 0.01$; ***, $P < 0.001$. Error bars indicate standard deviations. MFI, mean fluorescence intensity.

and evolutional divergence (68, 71). As shown in Fig. 8C, tetraspanins and L6 were expressed on the surface of 293T cells and did not modulate the surface expression of the other tetraspanin proteins (data not shown). Correlating with their surface expression, they were also efficiently incorporated into the released virions (Fig. 8D), as in the case of CD63 (Fig. 2). Furthermore, Magi assay revealed that CD9-, CD81-, CD82-, and CD231-enriched NL4-3 also had less infectivity (Fig. 8E). However, L6-enriched NL4-3 had infectivity comparable to that of typical NL4-3 (Fig. 8E). Interestingly, as found in the case of CD63, we also observed that virion-incorporated tetraspanins did not affect JR-FL infectivity (Fig. 8E). These results suggest that many tetraspanins have the potential to attenuate NL4-3 infectivity and that tetraspanins may cooperatively modulate its infectivity.

DISCUSSION

Various host membrane proteins, including CD63 and tetraspanin proteins, exist on HIV-1 particles (7, 9, 45, 46, 55), and some of them affect viral infection. For example, HLAs (6, 13, 44), costimulatory molecules (21, 25) and ICAM-1 (2, 4) enhance HIV-1 infectivity, while CD4 has the potential to suppress HIV-1 infection through incorporation into the released progeny virions (66). However, most of their functions for or against HIV-1 infection are still unclear. In this study, we quantitatively assessed CD63 incorporation into HIV-1 particles released from T cells and epithelial cell lines (Fig. 1 and 2) and examined its influence on the infectivity of the virions. In Molt4/IIIB cells, we found that a large quantity of CD63 was incorporated into the released particles (Fig. 1D). CD63 incorporation was reduced upon cellular activation (Fig. 1D), and this reduction was accompanied by increased infectivity (Fig. 1B). We showed that our CD63 exogenous expression model in 293T cells is useful for studying the relationship between CD63 incorporation and virion infectivity by demonstrating that pCD63-transfected 293T cells expressed amounts of surface CD63 (Fig. 2B) similar to those in nonactivated Molt4/IIIB cells (Fig. 1F) and that exogenous CD63 was also successfully incorporated into the released virions (Fig. 2D). Using this system, we showed that the infectivity of NL4-3 virions was not affected by released CD63 not associated with virus particles (Fig. 3). Rather, the infectivity of NL4-3 was inversely correlated with both the amount of virion-incorporated CD63 and the level of surface expression of CD63 (Fig. 4). In contrast to NL4-3 and IIIB, we found that JR-FL was resistant to CD63-mediated infectivity reduction (Fig. 5 and 6) and that Env determined the susceptibility to CD63 (Fig. 6). In

addition, virion-incorporated CD63 had the ability to impair HIV-1 entry without affecting the binding of Env to CD4 (Fig. 7). Furthermore, we found that other tetraspanin proteins, such as CD9, CD81, CD82, and CD231, all had the potential to be incorporated into released HIV-1 particles and to interfere with NL4-3 infection, as in the case of CD63, and that this potential is unique in tetraspanin proteins (Fig. 8). Taken together, these finding are the first indication that some host membrane proteins have the potential to modulate HIV-1 infectivity in a strain-specific manner through incorporation into released particles.

As shown in Fig. 1B, the infectivity of released HIV-1 virion was enhanced by Molt4/IIIB activation. Although the amounts of mature Env in released virions were comparable (Fig. 1C), we detected a decrease in the amount of virion-incorporated CD63 (Fig. 1D) and suspected that CD63 on virions has the potential to regulate HIV-1 infectivity. To confirm this possibility, we first attempted to decrease endogenous expression of CD63 through transfection with small interfering RNA against *cd63* in 293T cells. However, we could not detect significant differences in the infectivity of released HIV-1 virions (data not shown). We suspected that the lack of difference was due to the low level of endogenous CD63 in HIV-1 particles released from 293T cells (Fig. 2D), and we next planned to study its exogenous expression. Exogenous CD63 was successfully incorporated into the released particles (Fig. 2D). This level corresponded closely to the level of CD63 on IIIB virions released from nonactivated Molt4/IIIB cells (Fig. 1D; compare Fig. 2D) and also to the level described in a previous report (35). In addition, the amount of endogenous CD63 in NL4-3 particles released from 293T cells (Fig. 2D) also corresponded with that in IIIB particles released from PHA/PMA-activated Molt4/IIIB cells (Fig. 1D; compare Fig. 2D). Because the level of surface CD63 as well as incorporated CD63 was comparable between two systems (Fig. 1F and 2B), this 293T system was adequate to simulate the physiological phenomenon observed in Molt4/IIIB cells.

As shown in Fig. 2H, we detected attenuation of NL4-3 infectivity released from pCD63-transfected 293T cells. It has been reported that surface CD4 impairs Env incorporation and reduces the infectivity of the released virions (12, 42). Surface CD63 might also reduce the infectivity by affecting incorporation of Env. However, exogenous CD63 did not impair either Env maturation (Fig. 2A, top) or Env incorporation (Fig. 2A, bottom). On the other hand, Wyma et al. reported that immature HIV-1 particles are less active for fusion with target cell than mature particles (72). Exogenous CD63 might attenuate the maturation of HIV-1 particles. However, we found that Gag cleavage was successful (Fig. 2A, bottom). Recently, Ho et al. reported that a soluble recombinant LEL of CD63 has an ability to prevent HIV-1 infection (33), and we detected release of non-virion-associated CD63 into the culture supernatant of pCD63-transfected cells (Fig. 2A, bottom, rightmost lane). It was suspected that non-virion-associated CD63 released into the culture supernatant affected HIV-1 infection. However, non-virion-associated CD63 had no effect on HIV-1 infection (Fig. 3). Non-virion-associated CD63, which would be embedded on exosome/microvesicle-like components, may be inaccessible, as previously seen in the soluble recombinant LEL (33). As shown quantitatively (Fig. 2D) and visually (Fig. 2F), we detected the existence of CD63 on the released particles, and the amount was increased through exogenous expression (Fig. 2D and G). In addition, we observed that CD63ΔL preferentially localized at the cell surface (Fig. 4B) (34), while the whole amount was comparable to that of wild-type CD63 (Fig. 4A). Furthermore, CD63ΔL was additively incorporated (Fig. 4E) and then severely suppressed the infectivity of released virions (Fig. 4D). From these results, the amount of CD63 at the surfaces of HIV-1-producing cells clearly correlated with the level of CD63 in virions and inversely correlated with the infectivity of progeny NL4-3 virions. Accordingly, it appears that CD63 at the cell surface has a greater potential to be efficiently incorporated into released virions, which leads to the reduction in infectivity. This preference is reminiscent of positive correlation between the level of ICAM-1 surface expression on HIV-1-producing cells and the level of ICAM-1 in HIV-1 virions (54), although the effects elicited by respective embedded proteins were completely opposite.

It is known that the tetraspanin proteins have high homology in their structures and amino acid sequences (32, 62). Consistent with this observation, we found that exogenous tetraspanin proteins, such as CD9, CD81, CD82, and CD231, were also efficiently expressed at the cell surface (Fig. 8C) and can be incorporated into released NL4-3 particles and interfere with their infection (Fig. 8D and E). In contrast, a transmembrane protein called L6, which has four transmembrane domains but does not belong to the tetraspanin superfamily (68, 71), was also expressed at the cell surface and incorporated into the released particles (Fig. 8C and D) but did not affect HIV-1 infection (Fig. 8E). Actually, it has been reported that soluble LELs of other tetraspanin proteins, such as CD9, CD81, and CD82, also have the potential to suppress HIV-1 infection (33). Therefore, our findings clearly suggest that this is a common role for tetraspanins.

We observed that virion-incorporated CD63 did not affect JR-FL infectivity (Fig. 5B). In addition, through a pseudotyped-virus infection assay, we found that exogenous CD63 impaired the infection mediated by NL4-3 Env (Fig. 6A) and IIIB Env (Fig. 6B) in a dose-dependent manner and independently of the target cells (as shown in Fig. 6F, it was also confirmed in primary activated $CD4^+$ T cells). In contrast, there were no effects on the infection mediated by JR-FL Env (Fig. 6D) and VSV-G (Fig. 6E), although exogenous CD63 was incorporated into released particles in an Env-independent manner (Fig. 2E). These results indicate that susceptibility to CD63 is determined in Env and that there is strain specificity. There is a well-known difference between NL4-3 and JR-FL in their coreceptor usage: the former uses CXCR4 and the latter uses CCR5, and coreceptor preference is determined by the V3 region of Env (66). Since the infectivity reduction could be V3 region dependent, we further used NLFLV3 that contains the V3 region of JR-FL Env in NL4-3 Env and uses CCR5 as the coreceptor. However, the difference in the susceptibility for virion-incorporated CD63 between NL4-3 and JR-FL was not caused by the difference in coreceptor usage (Fig. 5B). Actually, other R5 viruses, such as JR-CSF and several chimeras, were also susceptible to CD63 (data not shown). In this regard, it is interesting that there is a difference in CD63 susceptibility between two R5 HIV-1 strains, JR-FL and JR-CSF, which were simultaneously isolated from the brain of an HIV-1 en-

cephalopathy patient (40). While the determinant region(s) in Env for the vulnerability to virion-incorporated CD63 has not been identified, these results indicate that there is some kind of strain specificity, or that JR-FL Env has some resistant property against virion-incorporated tetraspanins. It has been reported that a trivial change in Env conformation caused by mutation of one or more amino acid residues is responsible for the resistance to neutralizing antibodies and anti-HIV-1 drugs and that there are trivial differences in Env conformation between HIV-1 strains (5, 58). However, the crystal structure of the entire HIV-1 Env is not yet resolved, and it is difficult to speculate accurately on the invisible conformation of Env from its amino acid sequence. Our findings shed light on an unknown difference(s) between HIV-1 Envs, which is possibly conformational. Therefore, our findings may provide a clue for elucidating the ambiguous conformation of HIV-1 Env, which may lead to a novel target of anti-HIV drugs.

It has been reported that CD4 has the potential to inhibit HIV-1 infection at the attachment step through incorporation into the released HIV-1 particles (66). In contrast, as shown in Fig. 7A, virion-incorporated CD63 did not affect the attachment step. Rather, a postattachment step was attenuated by CD63 enrichment (Fig. 7B to D). It has been reported that the correct interaction between gp41 CT and $p17^{MA}$ in progeny virions is important to elicit efficient conformational changes of HIV-1 Env, leading to infection (14, 16, 72, 73). Virion-incorporated CD63 may disturb the interaction between gp41 CT and $p17^{MA}$ at the lining of virions. However, the infectivity of a CT-deleted NL4-3 Env-pseudotyped virus was also decreased by exogenous CD63 (Fig. 6C), suggesting that virion-incorporated CD63 had no or little effect on the interior of progeny virions. Interestingly, there are several reports showing that tetraspanin proteins are associated with physiological membrane fusion events. For example, murine CD9 on oocytes contributes to sperm-egg fusion (43, 47), and CD9 and CD81 on mononuclear phagocytes prevent their mutual fusion (65). In the case of human retroviruses, it was recently reported that the syncytium formation mediated by HIV-1 Env is suppressed by overexpression of CD9 and CD81 on the target cells (26). We think this is yet another phenomenon in which tetraspanin proteins are involved. Actually, tetraspanin proteins are able to interact laterally with each other through their LELs (62). Hence, CD63 on HIV-1 virion may laterally interact with endogenous CD9 and CD81 on target cells and may constitute an obstacle that impairs the stable interaction between gp120 and CD4/coreceptors following attachment.

Interestingly, PHA/PMA activation of Molt4/IIIB cells enhanced the infectivity of released IIIB virions (Fig. 1B), while the amount of incorporated Env was not changed (Fig. 1C). In this situation, it was interesting that the amount of virion-incorporated tetraspanins was decreased (Fig. 1D and 8B) and that their surface expression was significantly down-regulated (Fig. 1F and 8A). There was a clear relationship between the infectivity of released HIV-1 virions and the amount of tetraspanin proteins on both the virion and the surfaces of HIV-1-producing cells. Therefore, the enhancement of IIIB infectivity upon PHA/PMA activation of Molt4/IIIB cells should be at least partially due to the down-regulation of tetraspanin proteins.

Recently, the importance of tetraspanin proteins in HIV-1 replication has been recognized (3, 26, 50). The so-called "Trojan exosome hypothesis" proposes that HIV-1 applies TEMs and the machineries of exosome biosynthesis to its extracellular egress (27). However, the results we present here suggest that CD63 and other tetraspanins on viral membranes also have the potential to interfere with viral infection. The fundamental roles of tetraspanins and cellular membrane proteins in HIV-1 virions are intriguing, and further studies will be needed to uncover their mechanisms of action.

ACKNOWLEDGMENTS

We thank T. Murakami (AIDS Research Center, National Institute of Infectious Diseases), E. O. Freed (HIV Drug Resistance Program, National Cancer Institute-Frederick), Y. Ishizaka (Department of Intractable Diseases, International Medical Center of Japan), E. Mekada (Research Institute for Microbial Disease, Osaka University), W. A. O'Brien (Department of Microbiology and Immunology, University of Texas Medical Branch), and W. C. Greene (Gladstone Institute of Virology and Immunology, University of California) for providing materials required for this study. We are also grateful to the following colleagues from the Institute for Virus Research, Kyoto University, and Osaka Medical College: Yoshiharu Miura, Tomoko Kobayashi, and Yoshihiko Fujioka for instruction and support of experimental techniques, Youichi Suzuki for helpful suggestions, Chuanyi Nie for proofreading of the manuscript, and Takeshi Yoshida for lively discussions.

This work was supported by grants from the Ministry of Health, Labor and Welfare and the Ministry of Education, Culture, Sports, Science and Technology of Japan.

REFERENCES

1. **Adachi, A., H. E. Gendelman, S. Koenig, T. Folks, R. Willey, A. Rabson, and M. A. Martin.** 1986. Production of acquired immunodeficiency syndrome-associated retrovirus in human and nonhuman cells transfected with an infectious molecular clone. J. Virol. **59:**284–291.
2. **Beausejour, Y., and M. J. Tremblay.** 2004. Envelope glycoproteins are not required for insertion of host ICAM-1 into human immunodeficiency virus type 1 and ICAM-1-bearing viruses are still infectious despite a suboptimal level of trimeric envelope proteins. Virology **324:**165–172.
3. **Booth, A. M., Y. Fang, J. K. Fallon, J. M. Yang, J. E. Hildreth, and S. J. Gould.** 2006. Exosomes and HIV Gag bud from endosome-like domains of the T cell plasma membrane. J. Cell Biol. **172:**923–935.
4. **Bounou, S., J. E. Leclerc, and M. J. Tremblay.** 2002. Presence of host ICAM-1 in laboratory and clinical strains of human immunodeficiency virus type 1 increases virus infectivity and $CD4^+$-T-cell depletion in human lymphoid tissue, a major site of replication in vivo. J. Virol. **76:**1004–1014.
5. **Burton, D. R.** 1997. A vaccine for HIV type 1: the antibody perspective. Proc. Natl. Acad. Sci. USA **94:**10018–10023.
6. **Cantin, R., J. F. Fortin, G. Lamontagne, and M. Tremblay.** 1997. The presence of host-derived HLA-DR1 on human immunodeficiency virus type 1 increases viral infectivity. J. Virol. **71:**1922–1930.
7. **Cantin, R., S. Methot, and M. J. Tremblay.** 2005. Plunder and stowaways: incorporation of cellular proteins by enveloped viruses. J. Virol. **79:**6577–6587.
8. **Cavrois, M., C. De Noronha, and W. C. Greene.** 2002. A sensitive and specific enzyme-based assay detecting HIV-1 virion fusion in primary T lymphocytes. Nat. Biotechnol. **20:**1151–1154.
9. **Chertova, E., O. Chertov, L. V. Coren, J. D. Roser, C. M. Trubey, J. W. Bess, Jr., R. C. Sowder, I. I., E. Barsov, B. L. Hood, R. J. Fisher, K. Nagashima, T. P. Conrads, T. D. Veenstra, J. D. Lifson, and D. E. Ott.** 2006. Proteomic and biochemical analysis of purified human immunodeficiency virus type 1 produced from infected monocyte-derived macrophages. J. Virol. **80:**9039–9052.
10. **Choe, H., M. Farzan, Y. Sun, N. Sullivan, B. Rollins, P. D. Ponath, L. Wu, C. R. Mackay, G. LaRosa, W. Newman, N. Gerard, C. Gerard, and J. Sodroski.** 1996. The β-chemokine receptors CCR3 and CCR5 facilitate infection by primary HIV-1 isolates. Cell **85:**1135–1148.
11. **Cocchi, F., A. L. DeVico, A. Garzino-Demo, A. Cara, R. C. Gallo, and P. Lusso.** 1996. The V3 domain of the HIV-1 gp120 envelope glycoprotein is critical for chemokine-mediated blockade of infection. Nat. Med. **2:**1244–1247.
12. **Cortes, M. J., F. Wong-Staal, and J. Lama.** 2002. Cell surface CD4 interferes with the infectivity of HIV-1 particles released from T cells. J. Biol. Chem. **277:**1770–1779.
13. **Cosma, A., D. Blanc, J. Braun, C. Quillent, C. Barassi, C. Moog, S. Klasen,**